Relative Humidity Induced Plant Pollen Grain Rupture and Conceptual Model Development

By

Qian Zhou

A thesis submitted in partial fulfillment of
the requirements for the degree of

MASTER OF SCIENCE IN ENVIRONMENTAL ENGINEERING

WASHINGTON STATE UNIVERSITY
Department of Civil and Environmental Engineering

MAY 2014

To the Faculty of Washington State University:

The members of the Committee appointed to examine the thesis of QIAN ZHOU find it satisfactory and recommend that it be accepted.

_____

Timothy M. VanReken, Ph.D., Chair

_____

Brian K. Lamb, Ph.D.

_____

Serena H. Chung, Ph.D.

ACKNOWLEDGMENT

I would like to thank my advisor, Professor Dr. Timothy VanReken from the Laboratory for Atmospheric Research at Washington State University for his support, help, and suggestions. I would also like to express my gratitude to my committee members, Professor Dr. B. Lamb and Dr. S. Chung, and my great thanks to my group members: C. Faiola, R. Zhang, and M. Wen for their advice and help in the lab.

In addition, I would like to thank all of those at LAR and on campus that provided help; without them I could not have finished this thesis.

Finally, I would like to thank the EPA and CSC for their funding.

Relative Humidity Induced Plant Pollen Grain Rupture and Conceptual Model Development

Abstract

by Qian Zhou, M.S.
Washington State University
May 2014

Chair: Timothy VanReken

Asthma is a chronic respiratory disorder affecting millions of people. The disorder causes inflated bronchi and narrowed airways. Pollen particles are the critical allergens during pollination season. Pollen grains themselves are too large to enter the lower airways, but once the grains rupture, allergenic particles are released that can be inhaled. Understanding the conditions leading to pollen rupture is important in preventing allergen exposure in asthma patients. The main goal of this research is to identify the link between meteorological conditions and allergenic particles release following pollen grain rupture. The more specific objective is to identify the key driving factors behind pollen rupture and to develop a rupture mechanism model to predict pollen rupture in the natural environment.

Our main hypothesis is that pollen grains absorb water through water potential difference, causing the shell of the pollen grain to swell and rupture. We have investigated the relationship between pollen grain rupture and relative humidity (RH). Parameters from these experiments have been used to develop a model describing the pollen rupture mechanism.

A small humidity exposure apparatus has been built to quantify the dependence of pollen grain rupture on RH over time. Wheat pollen grains were used in the research. The results indicate that exposure to higher RH speeds pollen grain rupture and leads to a higher rupture fraction. To better understand the thermodynamics and kinetics of water flux and the change in water potential during pollen rupture, a rupture model is being developed using parameters from the experimental work. Because changes in the surrounding water potential modify turgor pressure inside the pollen grain, this rupture model will be used to describe the whole rupture mechanism. Rupture occurs as soon as turgor pressure exceeds the strength of the pollen grain shell. From the experimental results we speculate that the pollen rupture pattern is determined by the pollen's threshold water potential, the shell's water permeability, the strength of the pollen shell, the pollen grain radius, environmental RH, and exposure time.

TABLE OF CONTENTS

Page

ACKNOWLEDGMENT iii

Abstract iv

LIST OF TABLES viii

LIST OF FIGURES ix

CHAPTER 1 : INTRODUCTION 1

1.1Asthma 1

1.2 Pollen 3

1.3 Previous research 5

1.4 Chamber Experiment 10

CHAPTER 2 : CHARACTERIZATION OF RH CONTROL CHAMBER 15

2.1 Purpose of the Investigation 15

2.2 Exposure Chamber 16

CHAPTER 3 : WHEAT POLLEN RUPTURE EXPERIMENT 24

3.1 Purpose of Investigation 24

3.2 Rupture Experiment 24

3.3 Data analysis 26

3.4 Ryegrass experiments 33

CHAPTER 4 : RUPTURE MODELING DEVELOPMENT 35

4.1 Purpose of Investigation 35

4.2 Equation development 38

4.3 Assumptions..... 40

4.4 Two Stage Inflated Model 44

4.5 Simulated Results..... 46

CHAPTER 5 : CONCLUSIONS 54

BIBLIOGRAPHY:..... 56

LIST OF TABLES

Table 1. List of experiments with conditions 26

Table 2. Time of turgor pressure to start to increase and reach max pressure under RH=85%, 90%, 95% (with pollen radius of 25, 30, and 35 μm, and max expansion radius of 1 μm) 51

Table 3. Time of turgor pressure to start to increase and reach max pressure under RH=85%, 90%, 95% (with pollen radius of 25, 30, and 35 μm, and max expansion radius of 1.5 μm) 52

Table 4. Time of turgor pressure to start to increase and reach max pressure under RH=85%, 90%, 95% (with pollen radius of 25, 30, and 35 μm, and max expansion radius of 2 μm) 53

LIST OF FIGURES

Figure 1. Normal and inflamed lung and airway 1

Figure 2. Most flowers have four parts: sepal, petal, stamen, and pistil..... 4

Figure 3. SEM pictures of various pollen grains 5

Figure 4. The Bet v 1 allergens concentration released by birch pollen is related to rainfall and temperature change (Schäppi, Taylor et al. 1997)..... 7

Figure 5. Development of allergy 8

Figure 6. Schematic of chamber study by Taylor el al. (2002) from Caltech..... 11

Figure 7. Pollen particles distribution by Taylor et al. (2002)..... 12

Figure 8. Top view of Pan's chamber (2006) 15

Figure 9. Above: Schematic of exposure chamber (Unit: cm); Below: Exposure chamber with two glass slides as cover 17

Figure 10. Photo of exposure chamber on microscopic stage..... 18

Figure 11. Experimental Setup..... 19

Figure 12. Schematic of the experiment setup..... 21

Figure 13. Screen shot of LabVIEW controller..... 22

Figure 14. Picture of image capture system screen..... 23

Figure 15. Pollen images during a pollen rupture experiment (the above was captured near the start of the experiment; the below was captured near the end) 29

Figure 16. Pollen rupture fraction versus time for experiments at RH=90% 30

Figure 17. Pollen rupture fraction versus time for experiments at RH=85% 31

Figure 18. Cumulative pollen rupture fraction vs. time for all experiments..... 32

Figure 19. Red pine pollen experiments at RH=95% after 48 hours exposure..... 34

Figure 20. Water flux and turgor pressure changes in plant cells at various concentrations 36

Figure 21. One quarter of a plant pollen grain..... 37

Figure 22. Simulated turgor pressure change when K is increased by a factor of ten 41

Figure 23. Simulated turgor pressure change where K is decreased by a factor of ten 42

Figure 24. The discovery of a wheat pollen rupture threshold 44

Figure 25. Predicted pollen grain turgor pressure change over time (From above to below radius 25, 30, and 35 μm, max radius expansion 1 μm) 50

CHAPTER 1 : INTRODUCTION

1.1Asthma

Asthma is a common chronic human lung inflammatory disorder. Symptoms occur particularly at night and in the early morning and include wheezing, coughing, chest tightness, and difficulty breathing (Masoli, Fabian, Holt, Beasley, & Global Initiative for Asthma, 2004).

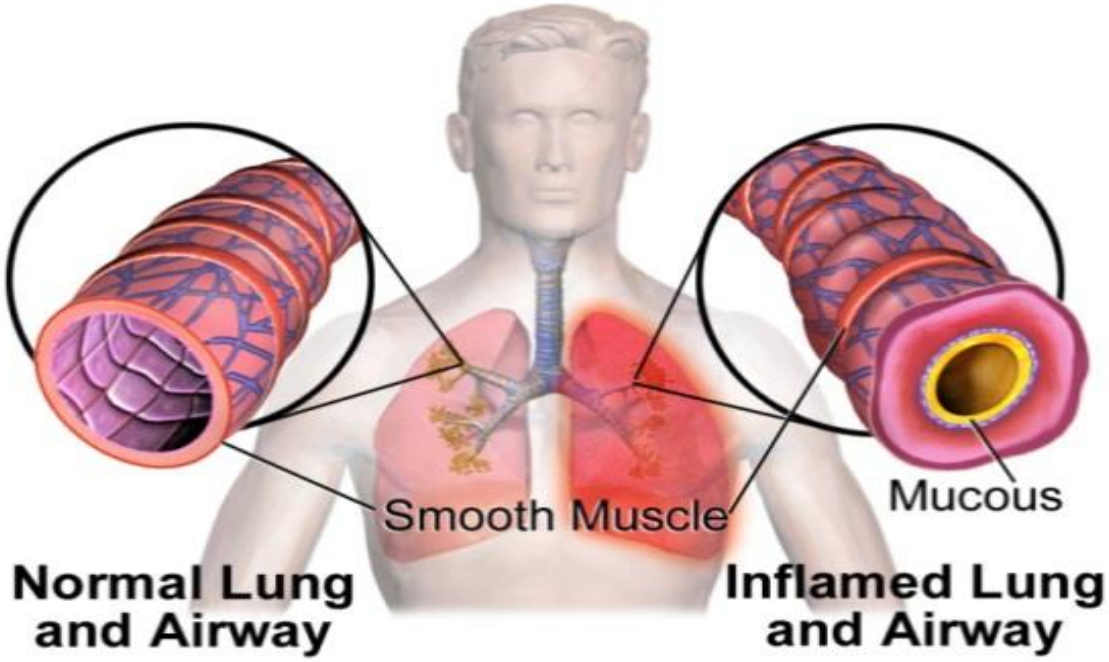

Figure 1. Normal and inflamed lung and airway

(http://www.niaid.nih.gov/topics/immunesystem/pages/disorders.aspx)

These symptoms are often associated with obstructed air flow in the lower bronchial airways. It is thought that asthma is complicatedly caused by a combination of genetics and environmental factors.

There is no clear definition of what exactly asthma is, but it is diagnosed based on the symptoms of each individual patient, especially those who have measurable factors and responses to environmental allergens. We know that asthma affects people of all ages throughout the world. In the United States, roughly twenty-two million people are affected by asthma. Worldwide, the number is more than three hundred million people and the global death toll from the disease is approximately 250 thousand each year (Masoli et al., 2004). Asthma rates, particularly in children, are rising in every country (Masoli et al., 2004).

Because asthma has no clear definition, it is difficult to compare the prevalence of the disease across countries or regions. Although the percentage of asthma patients varies (Masoli et al., 2004), the trend is upward, which means an increasing health burden. This increase is not only a burden in terms of insurance and health care costs, but also in terms of lost productivity and diminished well-being. A number of studies have focused on asthma in past decades (Celenza, Fothergill, Kupek, & Shaw, 1996; D'Amato, Liccardi, D'Amato, & Holgate, 2005; Masoli et al., 2004; Packe & Ayres, 1985; C. Suphioglu et al., 1992; P. Taylor & Jonsson, 2004). Research indicates that asthma can be treated effectively, and patients can relieve breathing difficulty and improve lung functions (Masoli et al., 2004). However, gaps exist in our understanding of environmental factors and their relationship to asthma. For example, exposure to air pollution or allergens can induce asthma, yet countries with severe air pollution may have a lower incidence of asthma than countries with cleaner air.

Reducing exposure to allergenic risk factors is the best way to control asthma (Masoli et al., 2004). Many factors are thought to contribute to human asthma, but the

most common risk factors include animal fur, dust mites, mold, and plant pollens (Masoli et al., 2004). Plant pollens have long been connected to asthma (P. Taylor & Jonsson, 2004), and the number of asthma cases often increase dramatically during plant pollen season (Celenza et al., 1996). Meteorological change is also associated with asthma, suggesting that pollen grains are affected by meteorological change (Pehkonen & Rantio-Lehtimäki, 1994). Thus, a connection between meteorological conditions, pollen grains, and asthma is likely.

1.2 Pollen

There are so many types and variations of plants in the world that it is impossible to find a good definition of *plant* that accurately excludes non-plants (Mukherjee & Litz, 2009). Generally, a plant can photosynthesize, store the energy from sunlight as glucose, and build polysaccharides and proteins for the plant body. Plants reproduce themselves in diverse ways and pass their genes onto the next generation; some grow beautiful flowers to produce seeds.

A flower is the sexual organ of diploid plants, which can produce haploid sex cells (including sperm and egg) through the process of meiosis. For the most part, flowers consist of a stem with leaf-like structures. Most flowers have four parts: sepal, petal, stamen, and pistil. Pollen is produced by the anther, which is part of the stamen. Four independent columns of tissue contain microspore mother cells. These cells continuously undergo meiosis and enlarge to produce tetrad-like microspores called pollen. These microspores are released into the environment as long as the anther is open.

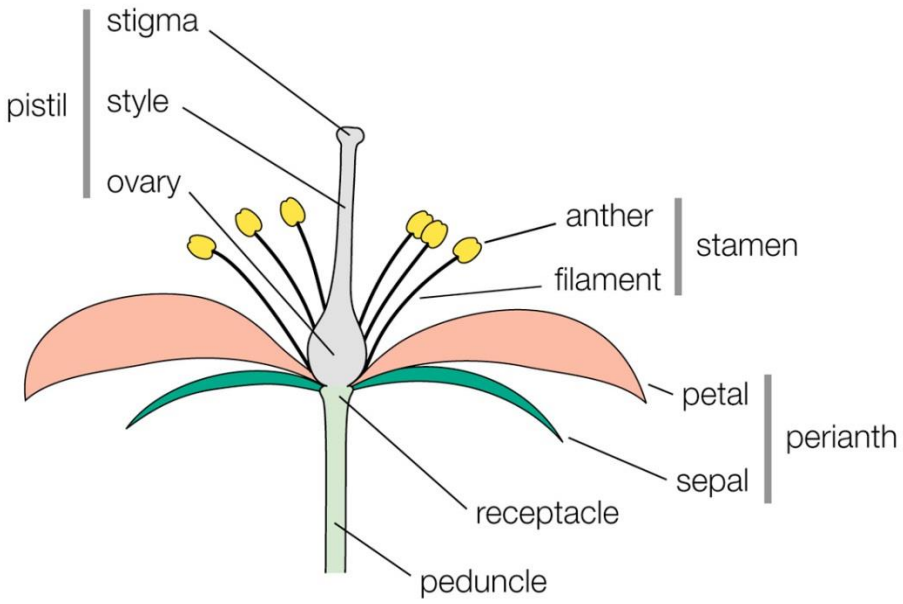

Figure 2. Most flowers have four parts: sepal, petal, stamen, and pistil

(Mauseth, 2009)

Pollen is a coarse powder containing plant seeds that produces male gametes (Fig. 3.). A hard wall protects the gametes inside a pollen grain. These are complex two-layer walls that are harder than most cell walls (Bolick & Vogel, 1992). The inner wall is called the intine and is made of cellulose; the outer layer, called the extine, consists mainly of the biological polymer sporopollenin. The wall consists of protein, lipids, and polysaccharides and resists adverse conditions in the natural environment. A pollen grain has one or several pores in the wall which are used to grow pollen tubes for fertilization. Once the pollen grains make contact with the stigma of the pistil, the male gametes begin to grow from a pore in the pollen grain shell.

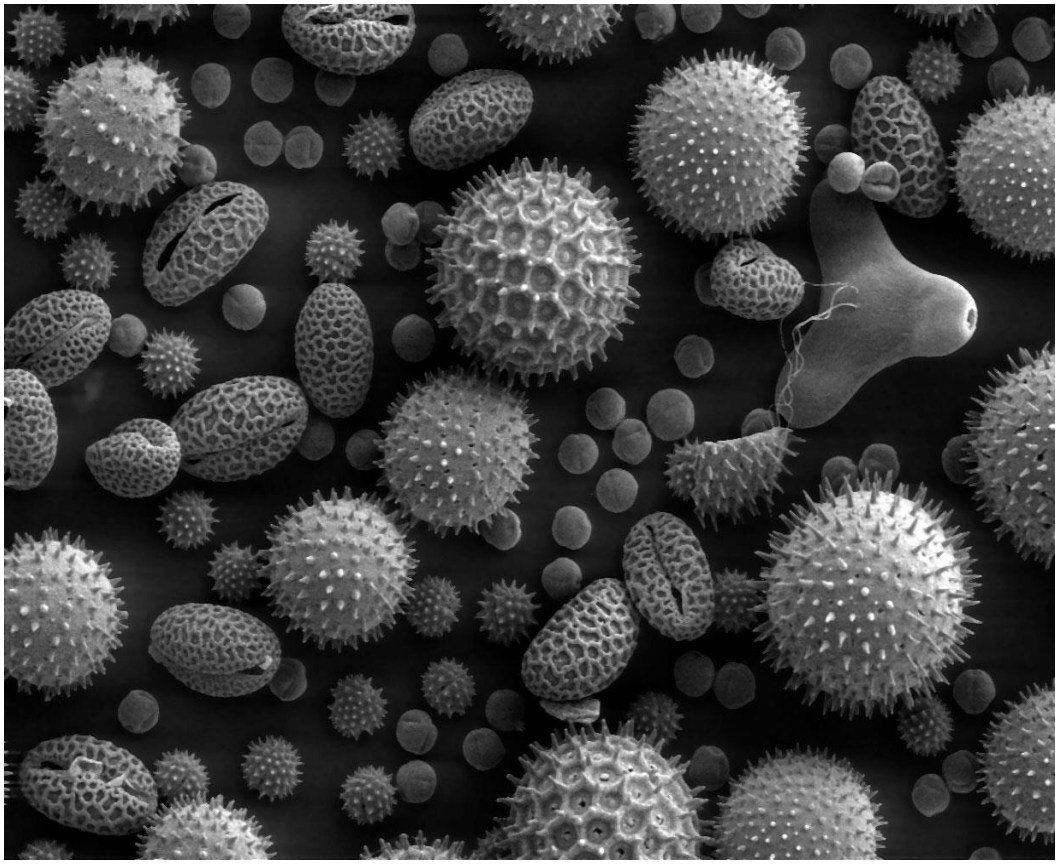

Figure 3. SEM pictures of various pollen grains

(http://upload.wikimedia.org/wikipedia/commons/thumb/a/a4/Misc_pollen.jpg/1009px-Misc_pollen.jpg)

1.3 Previous research

In the last century, before pollen was identified as a source of asthma allergens, the coincidental rise in asthma cases with precipitation was observed (Celenza et al., 1996; Dabrera et al., 2013; Pehkonen & Rantio-Lehtimäki, 1994; Cenk Suphioglu, 1998). One of the earliest such observations was reported by Packe and Ayres (Packe & Ayres, 1985), followed by Alderman et al. (Alderman, Sloan, & Basran, 1986), and Pehkonen and Rantio-Lehtimäki (Pehkonen & Rantio-Lehtimäki, 1994) who confirmed the

hypothesis that asthma is related to changes in meteorological conditions. Wardman et al. (Wardman, Stefani, & MacDonald, 2002) reported that during thunderstorms asthma patients accounted for five and seventeen percent of emergency room visits. On days without thunderstorms, the number was only one to two percent. It is interesting that in Wardman et al.'s study, males were more likely to experience acute asthma than females.

Only particles smaller than 5 μm can reach the lower respiratory airways (CHAN & LIPPMANN, 1980). Pollen grains (15-100 μm) are unable to move beyond the upper airways (Wilson, Novey, Berke, & Surprenant, 1973). Given this, for many years it was not clear how pollen could be connected to asthma. To reconcile this, Schäppi et al. (1997) suggested that pollen grains ruptured to release fragmented pollen particles and that the allergens were located in the pollen particles (Schäppi, Taylor, Staff, Suphioglu, & Knox, 1997). Precipitation can cause rupture of pollen particles, (Fig. 4).

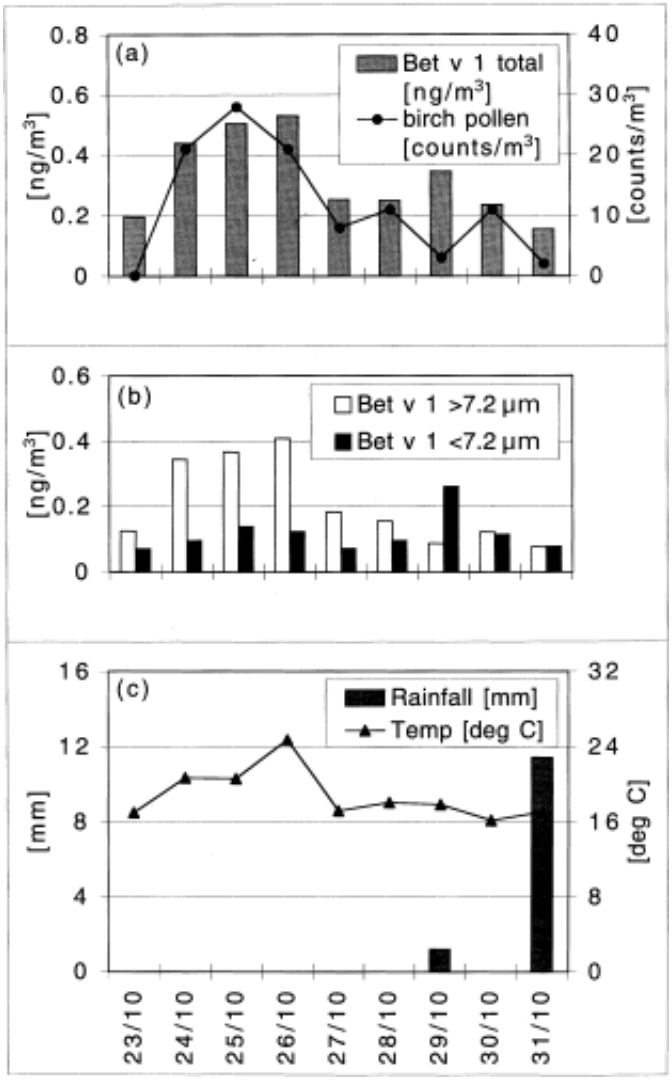

Figure 4. The Bet v 1 allergens concentration released by birch pollen is related to rainfall and temperature change (Schäppi, Taylor et al. 1997)

Previous research revealed that small pollen particles can be released after pollen rupture (C. Suphioglu et al., 1992). These particles contain allergens and can be inhaled by humans, causing asthma symptoms (Philip E. Taylor, Flagan, Valenta, & Glovsky, 2002). Rupture is associated with changes in meteorological conditions (Pehkonen & Rantio-Lehtimäki, 1994).

To confirm this, various pollen grains were immersed in water and then dried. (C. Suphioglu et al., 1992; Philip E Taylor, Jacobson, House, & Glovsky, 2007). Pollen was found to rupture when exposed to pure water, but the time to rupture varied considerably by pollen type. Grasses release more pollen than trees, and grass pollens rupture relatively quickly. Summarizing previous research, Taylor and his fellow researchers (Philip E. Taylor et al., 2002; Philip E Taylor et al., 2007) indicated that pollen could rupture and release asthma-related particles under saturated water vapor conditions.

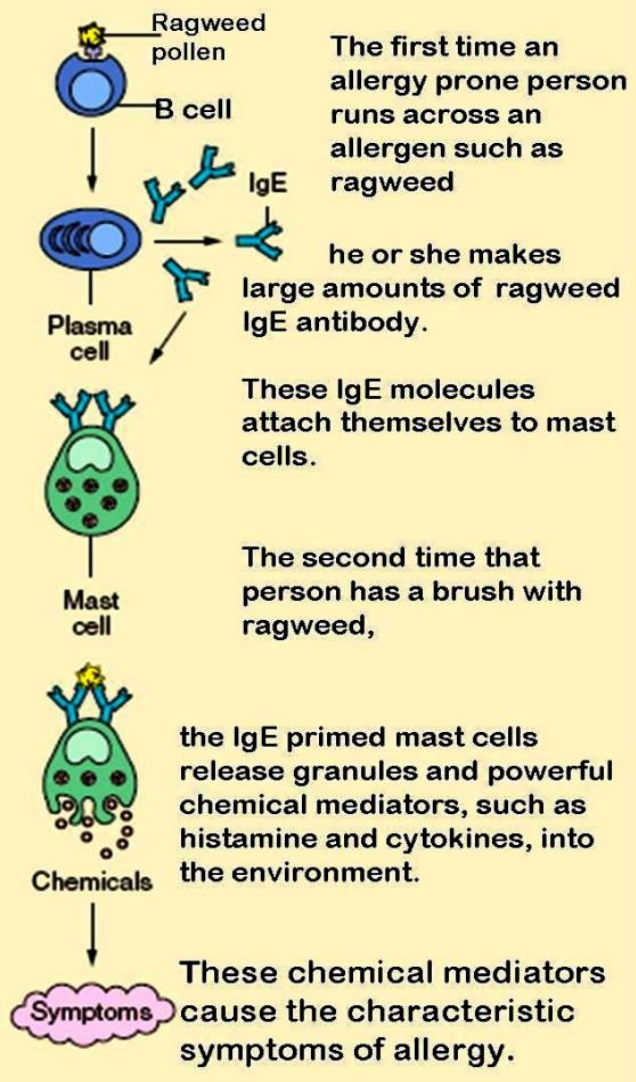

Figure 5. Development of allergy

The pollen particles released after rupture contain proteins, starch, and polysaccharides. Some of these materials are recognized by the human immune system which responds by producing antibodies against the invading particles (Fig. 5). Substances secreted by the immune system narrow the bronchial airways and make breathing difficult. (Fig. 5 . http://en.wikipedia.org/wiki/File:Mast_cells.jpg).

Immunoglobulin E (IgE) is a class of antibody found only in mammals. Increased IgE levels and elevated IgE sensitization to allergens in serum are central features of allergic asthma. The IgE level induced by pollen grains or particles can be evaluated by enzyme-linked immunosorbent assay (ELISA) (Abou Chakra et al., 2009), which identifies antigens using antibodies and color change. Studies have suggested that pollen particles could trigger more severe allergenic responses than the whole pollen grain. Animal experiments have indicated that pollen particles deeply penetrate the respiratory tract and induce strong allergic and inflammatory responses (Rogerieux et al., 2010). Pollen allergens were localized in the cytoplasm fragment after pollen grain rupture by Grote et al. (Grote, Vrtala, Niederberger, Valenta, & Reichelt, 2000). These studies suggest that asthma related allergens are located in pollen cytoplasm and can be released by pollen rupture under wet conditions or exposure to pure water. The particles are small enough to be inhaled and reach the lower airways. Immune assays have shown that these allergens can cause immune reactions and increase the level of IgE to produce strong allergic reactions in both *in vitro* and *in vivo* animal tests.

Pollen rupture and particle release has been studied for decades (Abou Chakra et al., 2009; Celenza et al., 1996; Packe & Ayres, 1985; Pehkonen & Rantio-Lehtimäki, 1994; Schäppi, Taylor, Staff, Rolland, & Suphioglu, 1999; Schäppi et al., 1997; Cenk Suphioglu, 1998; C. Suphioglu et al., 1992; P. E. Taylor, Flagan, Miguel, Valenta, & Glovsky, 2004; Philip E. Taylor et al., 2002; Wilson et al., 1973). Research demonstrated that pollen particles are the critical sources of asthma allergens (C. Suphioglu et al., 1992). Observations have suggested that pollen particles could be released by pollen grains during rainfall or thunderstorms (C. Suphioglu et al., 1992). However, pollen

grains from various plant species performed differently under the same subsaturated conditions (Philip E Taylor et al., 2007), indicating a strong probability that pollen grain rupture is related to both outside factors, such as changes in water vapor, and internal factors, such as the structural strength of the pollen grain shell.

Under what conditions a pollen grain ruptures and releases allergenic particles remains unknown, but it is clear that potential asthma patients should avoid outside activities to reduce exposure to pollen allergens under wet meteorological conditions during the pollination season.

The driving force behind pollen rupture also remains unclear. It is speculated that pollen rupture is closely related to changes in water vapor in the environment (Bolick & Vogel, 1992; C. Suphioglu et al., 1992). The pollen of many plant species will rupture under osmotic shock (such as during rain and thunder storms) (Celenza et al., 1996; Pehkonen & Rantio-Lehtimäki, 1994; Cenk Suphioglu, 1998; P. Taylor & Jonsson, 2004). However, pollen grains exposed to other subsaturated conditions over time may also rupture. This phenomenon leads us to seek the real reason behind pollen rupture.

This study proposes that the process of pollen grain rupture can be modeled in terms of osmotic pressure swell mechanics. In addition, we will quantify the dependence of pollen grain rupture on water vapor pressures over time. A rupture mechanics conceptual model will be developed to describe the pollen rupture mechanism, the kinetics of water flow, and the process of pressure change.

1.4 Chamber Experiment

Other studies (Pan, 2006; P. E. Taylor et al., 2004; Philip E. Taylor et al., 2002; Philip E Taylor et al., 2007; Vaidyanathan, Miguel, Taylor, Flagan, & Glovsky, 2006) indicate that a chamber is useful in investigating the impact of water vapor on pollen rupture. A small chamber will be built to control relative humidity (RH) and mimic changes in environmental water vapor conditions, and to obtain pollen rupture data associated with the water vapor changes. Taylor et al. (P. E. Taylor et al., 2004; Philip E. Taylor et al., 2002) built a two-foot-scale acrylic exposure chamber to study ryegrass and birch pollen grains rupturing under saturated and subsaturated conditions (Fig. 6).

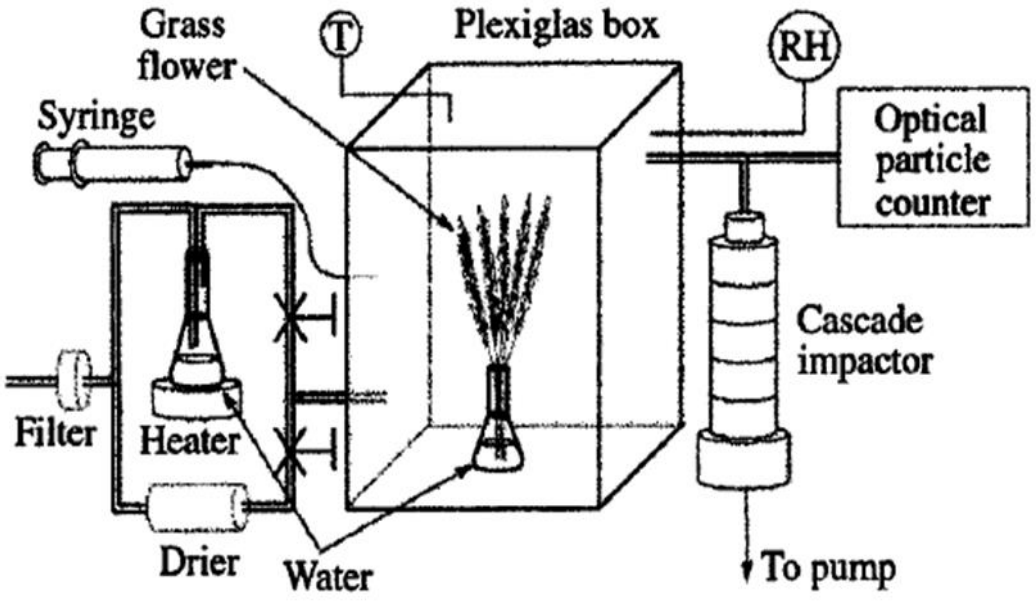

Figure 6. Schematic of chamber study by Taylor el al. (2002) from Caltech

Saturated RH was maintained in the exposure chamber to induce pollen rupture. The pollen particles were found to be released by the anther below 88% RH. Above 88%, the anther closes and pollen rupture occurs inside anther. This can be explained by the relationship of pollen rupture to high water vapor. The Taylor chamber was large enough

to hold tree branches and grass plants in a vase. The opening of the anther and the release of pollen grains under a variety of RH could be photographed. A downstream cascade impactor after chamber exposure was used to determine particle size and number (Fig. 7).

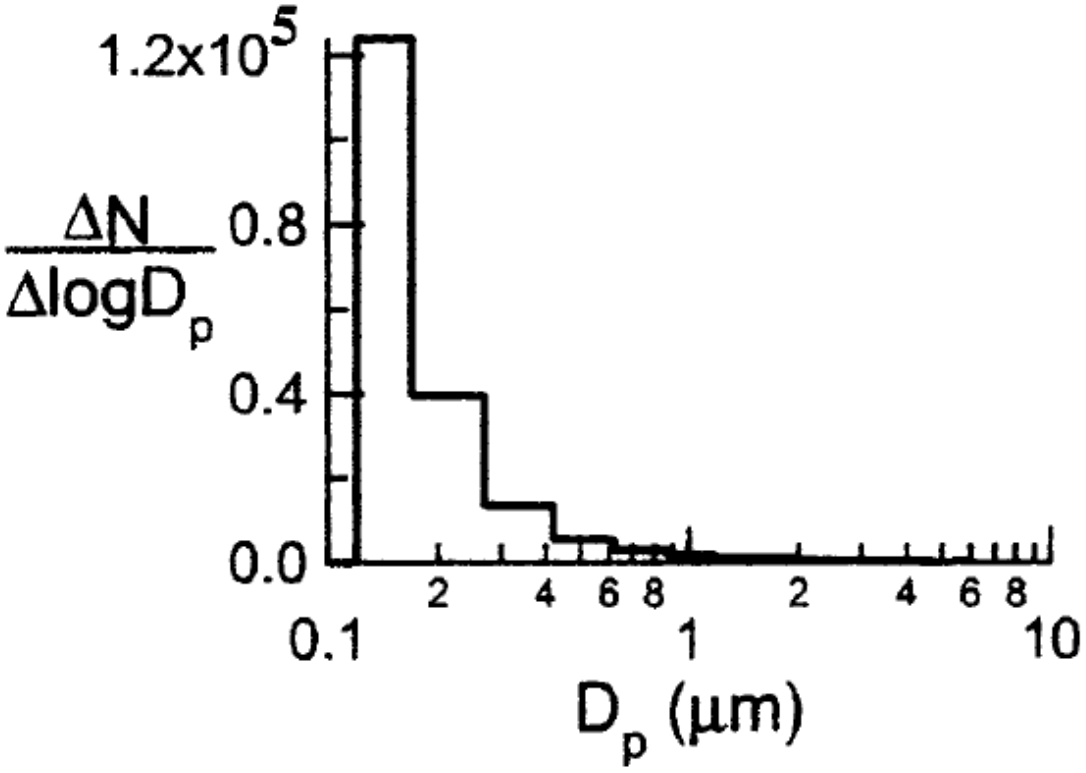

Figure 7. Pollen particles distribution by Taylor et al. (2002)

In Taylor et al., pollen ruptured under saturated and high subsaturated water vapor conditions. The released particles ranged from 0.1 to 5 μm in size and are group 1 allergens. These particles are small enough to be inhaled by humans and deposited in the lower airways. One drawback of Taylor's system was the lack of time-lapse image capability, preventing quantification of variations in pollen rupture with changes in water vapor. Another limitation of the study is that plant anther could open only under certain RH; if pollen grain rupture occurs only at different RH, then no particles could be

detected. This could prevent discovery of precise RH condition that leads to rupture. One additional limitation of the chamber was the large size, making RH maintenance slow and inaccurate, with substantial deviation. Our study indicated that pollen rupture was very sensitive to RH change. A large chamber would have greater RH fluctuations and the equilibrium state would be delayed, potentially resulting in the erroneous finding that pollen can rupture only under a higher RH. An electric field exposure chamber was built by Pan (Pan, 2006) in her bachelor thesis to observe plant pollen grain rupture under various electric fields. Pan's chamber was smaller than Taylor's and could be mounted on a microscope stage for image acquisition and analysis. The combination of these two chamber designs (Taylor and Pan) could be ideal for studying the impact of water vapor on pollen rupture and the dependence of rupture on RH exposure over time.

The remaining problem is how to identify the driving force behind pollen rupture. Previous research has indicated that water vapor pressure was significant in pollen rupture; however, other factors are likely involved and further investigation is needed. We hypothesize that water vapor pressure, pollen grain shell strength, and cytoplasm solution concentration are critical in pollen grain rupture. This investigation will rely on precisely-controlled RH exposure and systematic quantification of dependence of pollen rupture on water vapor exposure over time.

A real-time imaging system is needed to acquire pictures to simultaneously compare pollen grain rupture and RH changes. This requires an apparatus capable of controlling RH over long periods while maintaining the pollen sample in focus. A small pollen exposure chamber, roughly the size of a microscope slide, has been designed to accomplish this. Our experiments indicated that the pollen rupture pattern is highly

dependent on plant species; even different cultivated varieties could have diverse results. This phenomenon attracts our interest in studying the precise mechanism of rupture. We also are developing a rupture model using the parameters identified by the rupture experiment to explain and predict the mechanism of pollen grain rupture and allergen particle release.

CHAPTER 2 : CHARACTERIZATION OF RH CONTROL CHAMBER

2.1 Purpose of the Investigation

Relative humidity is the ratio of actual water vapor pressure to the saturated water vapor pressure at a given temperature. The best way to control the RH of ambient air is to build a chamber and mix dry air with humid air. A previous study (Taylor et al. 2002) built a desktop size chamber large enough to hold the branch of a birch plant. However, it is difficult to maintain precise RH in a large chamber. This study, for the first time, conquers the problem of a microscopic stage not fitting an RH exposure chamber, and successfully captures images of pollen rupture through a microscope.

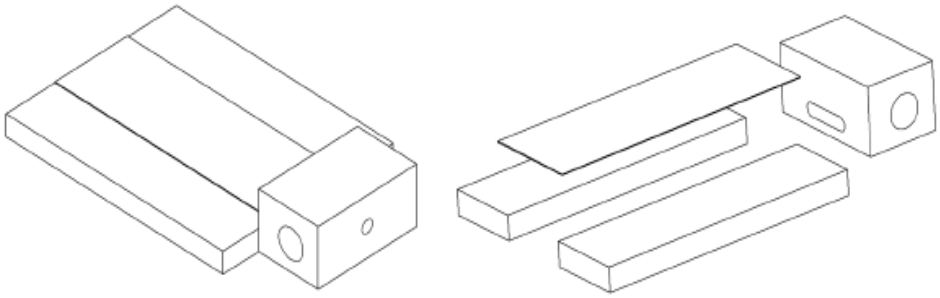

Figure 8. Top view of Pan's chamber (2006)

Studying pollen grain rupture at the microphysical scale requires an apparatus that allows observation of individual pollen grains under the desired experimental conditions to quantify the relationship between RH and pollen grain rupture. In this study, we determine under what subsaturated conditions pollen grains rupture. The proposed research is creative and unique, yet based on similar research (Figs. 6 and 8) (Pan, 2006;

Philip E. Taylor et al., 2002): the exposure chamber can be mounted on a microscope stage, allowing us to capture pollen images as the experiments proceed. Our research will has: 1) developed an apparatus to control RH exposure of pollen grains and acquire pollen rupture images; 2) captured images of pollen grain rupture and plotted the dependence of pollen grain rupture over time; 3) estimated water permeability and pollen RH threshold; 4) initial development of a rupture model showing that pollen grain rupture is dependent on RH over time.

2.2 Exposure Chamber

A microscopic exposure chamber has been built based on the idea from Pan's thesis (Pan, 2006) (Fig. 8), but we have modified the electric field device to control RH while enabling image capture. The main body of the exposure chamber is a rectangular U-shaped aluminum frame, with slots for the insertion of two glass microscope slides as the top and bottom covers. The dimension of the chamber frame is 7.5 cm long, 3.3 cm wide and 1.25 cm high (Fig. 9a). After the two microscope slides are in place, the chamber is complete (Fig. 9b).

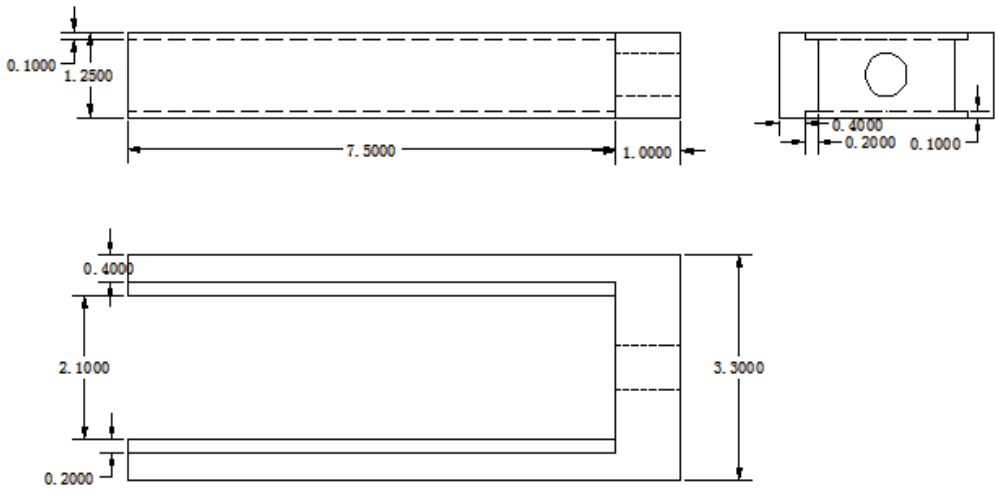

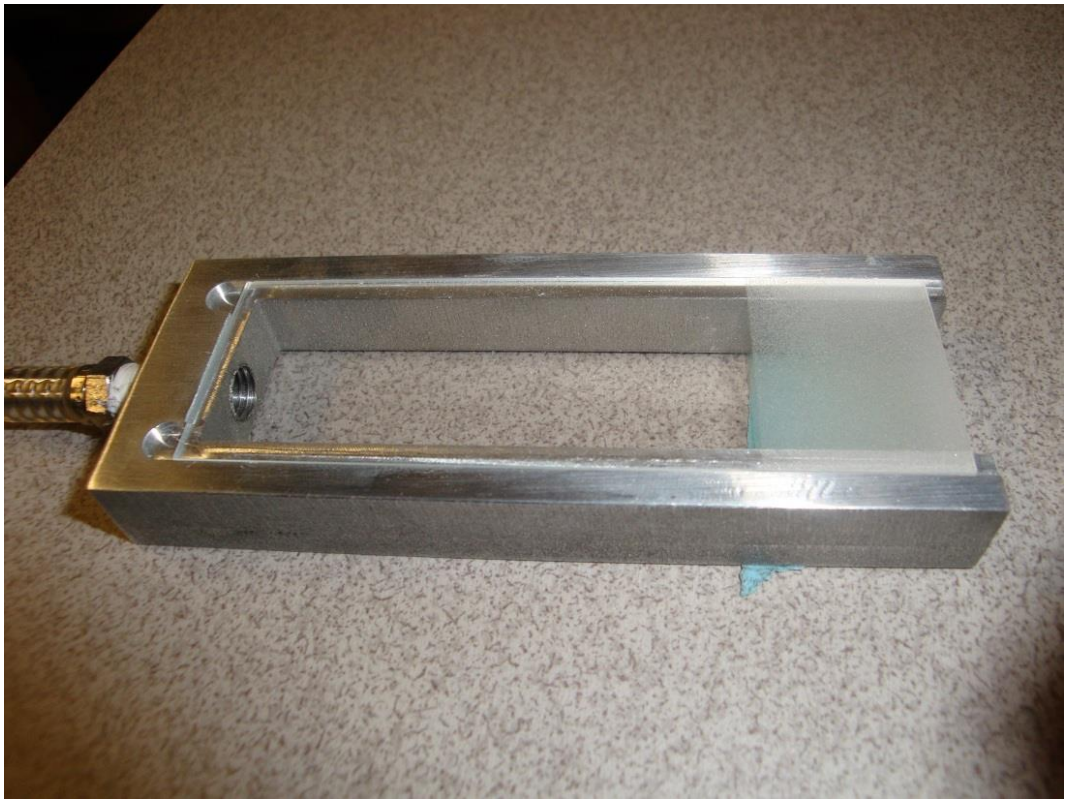

Figure 9. Above: Schematic of exposure chamber (Unit: cm)； Below: Exposure chamber with two glass slides as cover

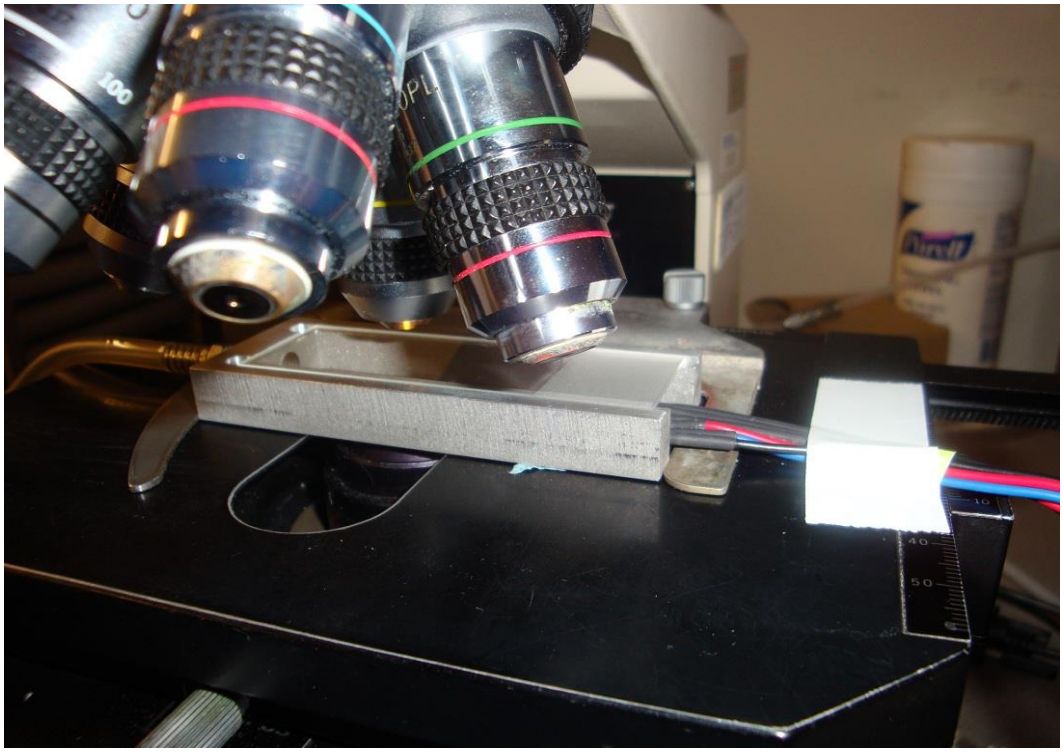

Figure 10. Photo of exposure chamber on microscopic stage

Humidity in the exposure chamber is controlled by passing a constant air flow into the chamber through a hole of 0.5 cm diameter at a rate of 0.2 L/min; the other end of the chamber is open to the room (Fig. 10).

Dry air flows originate from a compressed air cylinder. After passing through the volumetric flow controller (Alicat Scientific, Tucson, AZ) the air flow is humidified, up to 97% (humidifier's spec), using a Nafion humidifier (Perma Pure LLC, Toms River, NJ) before recombining it with a second dry air flow (Fig. 11&12). The black line in Figure 12 indicates air flow, while the red line is the electric signal for data acquisition. The blue line is the deionized water flow for the humidifier. This humidification system is actively regulated using LabView control software (National Instruments, Redmond, WA). One set of RH and temperature sensors (HMP110, Vaisala, Finland) is located in-line

immediately after the two air flows are mixed, and the other is within the glass slide chamber itself.

Figure 11. Experimental Setup

The light of the microscope lamp will be transmitted into the exposure chamber through two layers of glass slide and into the objective lens. The exposure chamber will trap some of the energy from the microscope lamp, raising the chamber temperature. This process will result in the saturated water vapor pressure increasing in the exposure chamber and decreasing the RH. Since RH control is based on the data collected from the RH sensor in the airstream line immediately after mixing the humid and dry air, the real chamber RH is lower than the expected RH value. To offset this bias, an AC fan is used

to cool down exposure chamber. However, this method is not accurate. Factors including the distance between exposure chamber and fan, the direction of the cooling fan towards chamber, and the height of the fan need to be determined and adjusted each time before the experiments start.

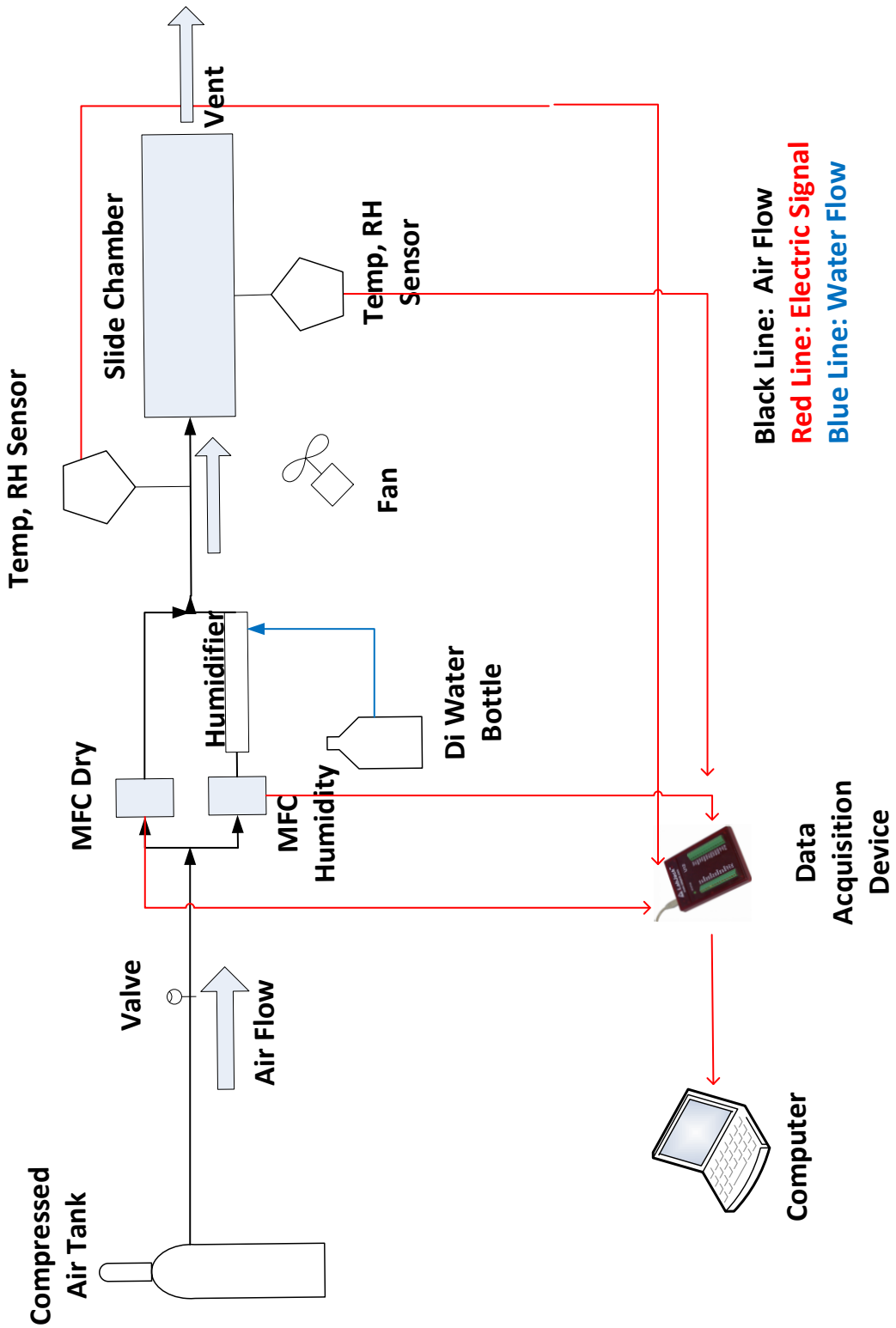

Figure 12. Schematic of the experiment setup

The main data acquisition is temperature and RH change, along with the images taken by a camera. The temperature and RH data are stored by LabVIEW (Fig. 13) and the pollen images are generated by the image capture software ProgRes.

The microscope's (Olympus BH-2 light microscope) objective lens magnification is 4x and the camera eyepiece is 2.5x, yielding a 10x total magnification. The microscope and attached camera (Jenoptik ProgRes C12 plus) are connected to a computer and a software (ProgRes 2.8.8) is used to record time-lapse images. The focus area is adjusted to have a maximum number of pollen grains in view. The view is locked throughout the experiment. Due to the length of the experiments, up to five hundred images can be recorded in each individual experiment. Images are saved in JPEG format with a resolution of 2,580 by 1,944 dpi (Fig. 14).

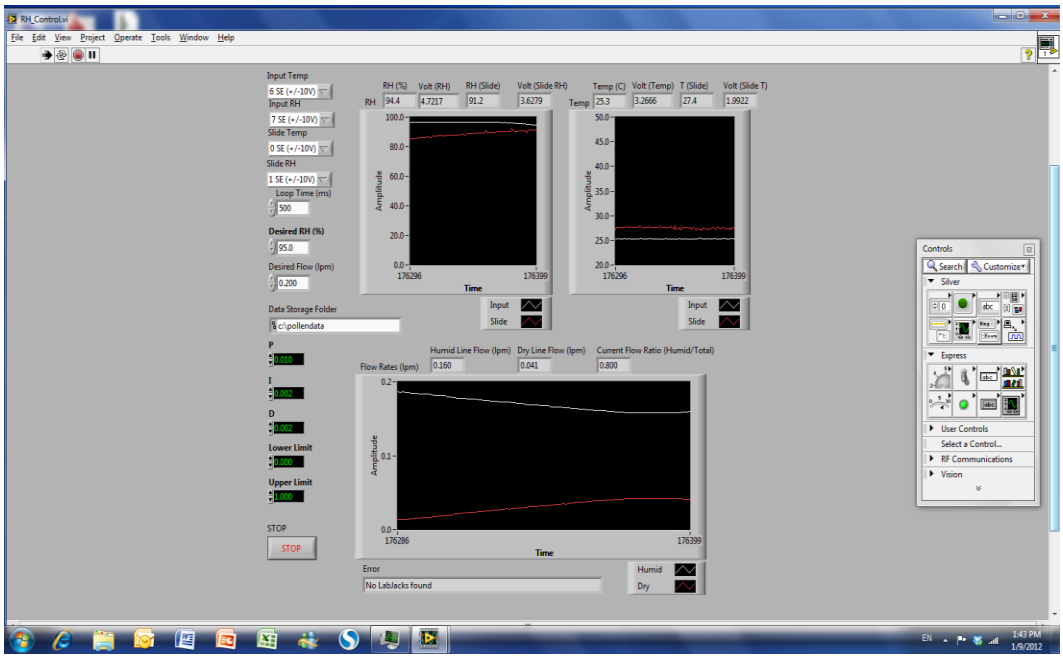

Figure 13. Screen shot of LabVIEW controller

.

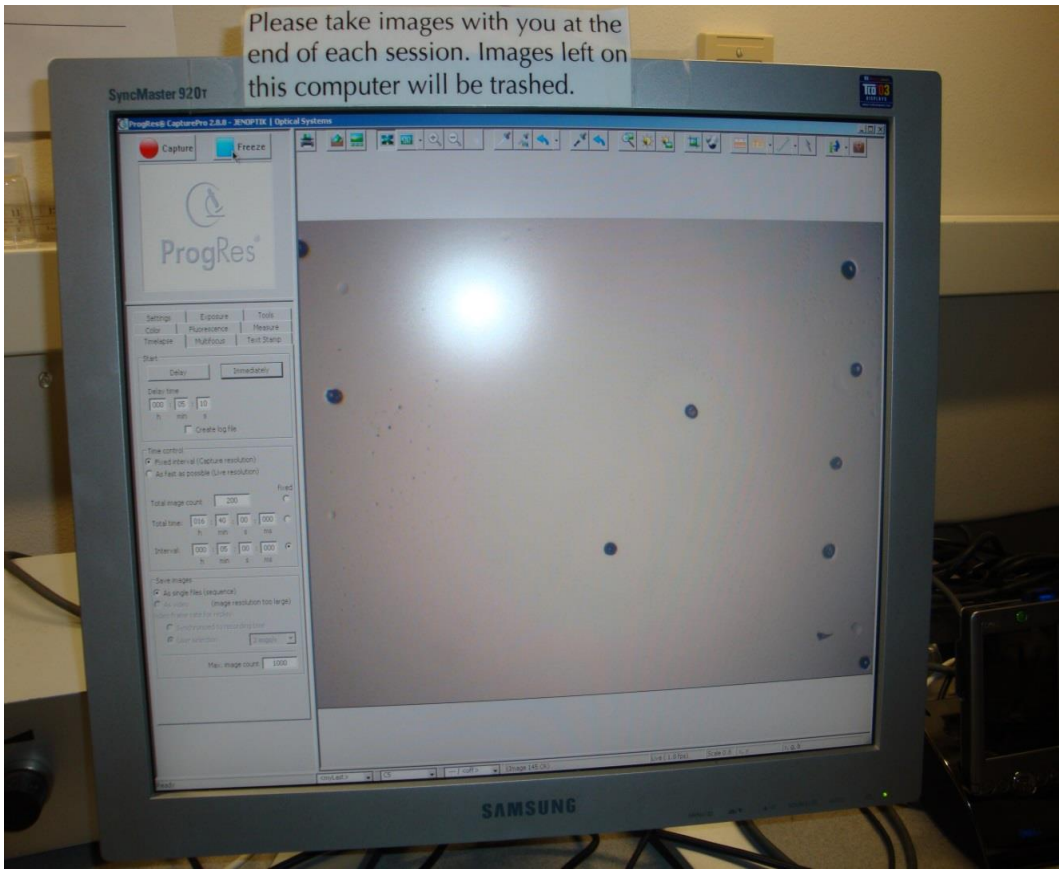

Figure 14. Picture of image capture system screen

CHAPTER 3 : WHEAT POLLEN RUPTURE EXPERIMENT

3.1 Purpose of Investigation

The purpose of this investigation is to test the capability of our chamber setup and collect data for rupture model development. The initial study with the pollen exposure chamber focused on wheat (*Triticum aestivum*) pollen grains. This was a practical choice because wheat is extensively studied at Washington State University (WSU), and flowering wheat heads are nearly always available year-round at the WSU greenhouse facility.

3.2 Rupture Experiment

At the start of each experiment, several fresh flower heads were collected from the WSU greenhouse. Flowering is regulated by temperature, and high temperature can reduce pollination kernel number and pollen viability (BarnabÁS, JÄGer, & FehÉR, 2008). Due to high temperature and the wheat's intensive transpiration at noon, the ideal time to gather pollen grains for the experiment is early morning and late afternoon.

To initiate the experiment, air flow with the desired RH was passed through the exposure chamber for at least thirty minutes to allow the system to reach equilibration. The microscope lamp was on during this period to increase the temperature of the exposure chamber and decrease the RH. An external cooling fan was turned on at the same time to offset the temperature increase; this allowed the temperature at the microscope stage to stabilize and minimize RH fluctuations during the experiment. As the system stabilized, the top slide of the exposure chamber was removed, and the pollen grains were shaken onto a fresh new glass slide. The glass slide was then inverted and

replaced on the top of the chamber with the pollen grains inside. This process should be fast and gentle—too long will destabilize the chamber humidity, and too much vibration reduces the number of pollen grains in the field of view. Once inside the chamber, the pollen grains stick to the inverted slide by Van der Waals forces and remain in place for the duration of each experiment. Because humid air continually entered the chamber and the chamber temperature was near steady state, only a short time was needed for re-equilibration after the pollen grains were added to the chamber. At this point the apparatus was left alone, with time-lapse images captured at five-minute intervals. Experiments continued until the pollen grains stopped rupturing—up to 48 hours.

Despite efforts to maintain precise RH control within the exposure chamber, in some experiments we found evidence of RH fluctuations. In the final analysis, we applied a screening standard to remove these flawed experiments. We set the filter with two conditions: 1) the mean chamber RH should be within 2% of the desired RH; and 2) the standard deviation of the chamber RH should be less than 1.5% during each individual experiment. Table 1 contains nine experiments data from RH=85% to RH=90%. RH becomes difficult to control when it is over 90%, especially at 95%. The fluctuation of RH at 95% will be greater than the filter standard, and all pollen grains rupture before the RH is stable. No pollen rupture has been observed when exposed to RH=80% or lower.

Table 1. List of experiments with conditions

Experiment ID	Target RH(%)	Achieved RH(%)	Temperature(℃)	Duration(min)	Pollen Grains#	Rupture Fraction
RH85-1	85	84.9±0.6	22.2	2860	25	92.0%
RH85-2	85	85.7±0.9	22.1	2760	23	95.6%
RH85-3	85	84.6±0.9	21.5	2920	20	65.0%
RH85-4	85	84.6±0.6	21.0	2870	16	87.5%
RH90-1	90	90.7±0.8	22.0	2880	28	92.8%
RH90-2	90	90.0±0.8	27.8	1525	26	80.7%
RH90-3	90	90.2±1.5	28.5	1020	12	91.7%
RH90-4	90	90.3±1.1	22.0	1155	25	76.0%
RH98-1	95	98.5±1.5	27.3	840	12	100%

3.3 Data analysis

The images were analyzed individually and automated, in sequence, to track the rupture of each pollen grain as time elapsed. To facilitate this arduous task, images were first preprocessed using Igor Pro for improved visual clarity. By examining the difference in two sequential pictures, we determined whether or not the pollen grain had ruptured during that interval (Fig. 15). If a rupture event was found to have occurred, the time and location of the event are recorded. After all of the pictures in an experiment were viewed and analyzed, the fraction of grains ruptured was calculated and plotted versus elapsed

time. However, the difference between two sequential images is small and difficult to distinguish. In Fig. 15, one image at the beginning of the experiment and one image near the end of the experiment are used for demonstration.

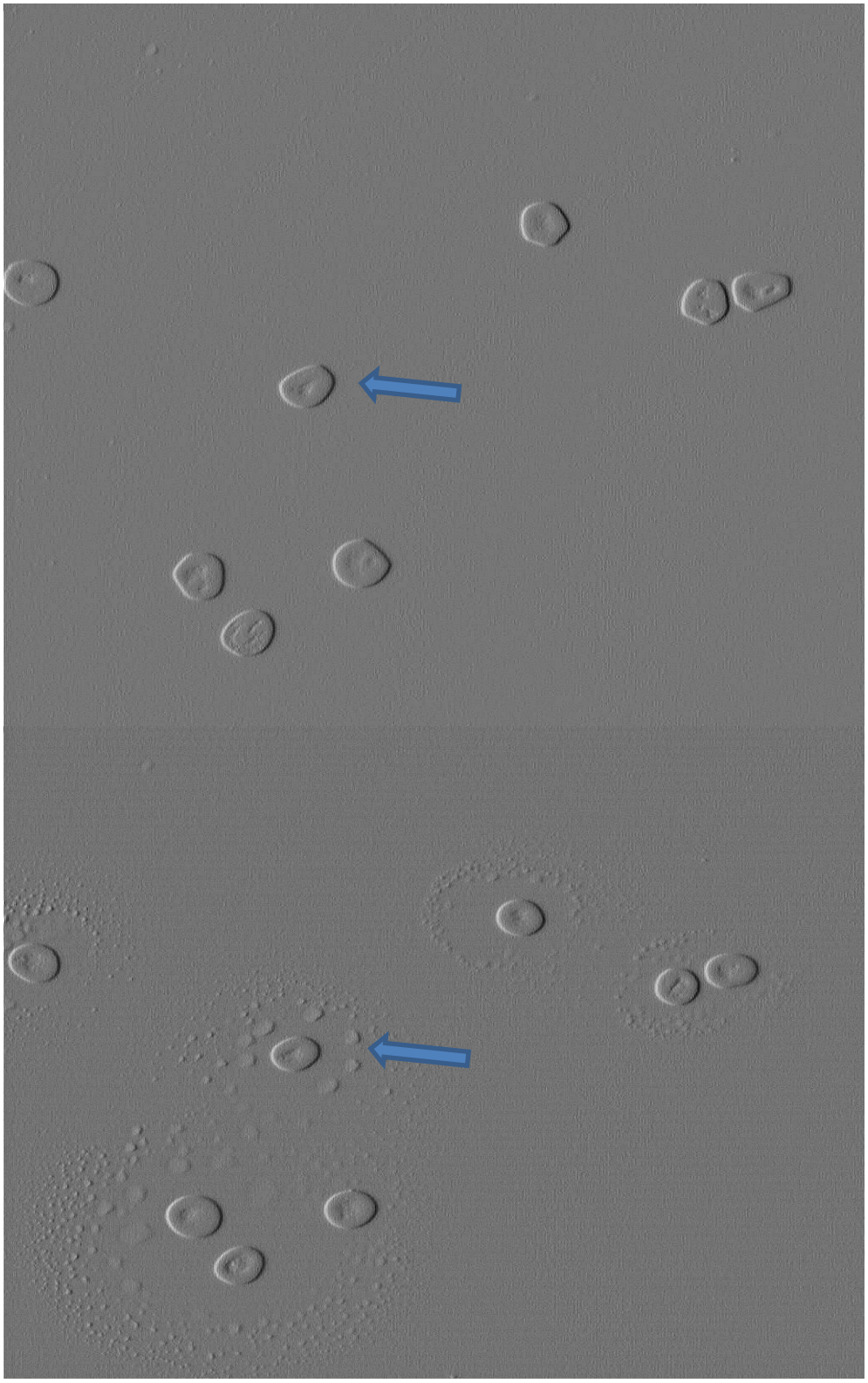

Figure 15. Pollen images during a pollen rupture experiment (the above was captured near the start of the experiment; the below was captured near the end)

The initial experiments started at RH=45% with a 5% RH increment, no rupture was observed in any of several experiments until RH=85%. Wheat pollen loses moisture and desiccates quickly when exposed to RH of below 85%. The lower the RH exposure, the faster the pollen grains shrink. Thus no wheat pollens rupture below RH=85%. We hypothesized that there is a threshold for pollen rupture to occur. When the ambient RH is above the threshold RH, pollens rupture; however pollen does not rupture if the RH is below the threshold. Because of the specifications of our sensors and control device, it is difficult to maintain RH with low deviation. Once the RH was above 90%, the deviations increased and were more difficult to maintain. Particularly above 95%, the RH fluctuated and sometimes the experiments stopped. However, at RH=95%, the pollen ruptured quickly. Even before the PID control maintained a stable RH, all of the pollen grains ruptured. We, therefore, shifted the experiment back to 85% and 90%. Numerous experiments were conducted at RH = 85% and RH = 90%. Many failed to meet the RH design criteria and were excluded. The remaining experimental results showed significant variability with respect to the rate of rupture and total fraction ruptured (Figs. 16 and 17).

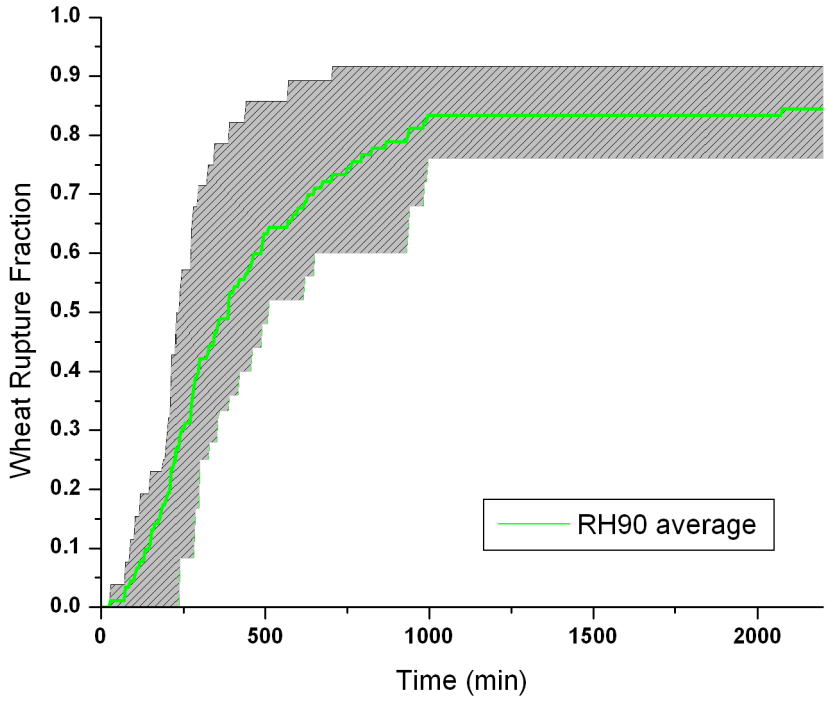

Figure 16. Pollen rupture fraction versus time for experiments at RH=90%

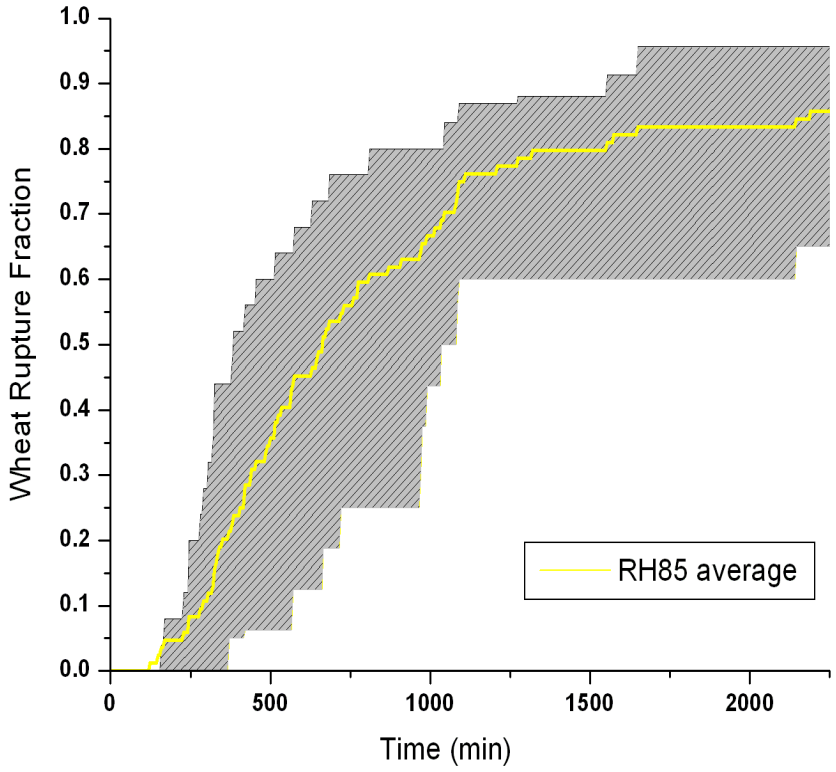

Figure 17. Pollen rupture fraction versus time for experiments at RH=85%

The pollen rupture fraction at RH=85% (Fig. 17) had greater variation (shadow area), indicating that water the potential in the water vapor was close to the water potential in the pollen grain cytoplasm. The water flux from air at RH=85% to pollen grain is smaller than at RH=95%, and therefore took longer to rupture. The average rupture fraction at RH=85% and RH=90% were close, but we could see a difference by plotting the cumulative fraction rupture (Fig. 18). Although each individual plot had a varied rupture pattern, the cumulative plot indicated that pollen rupture occurred more quickly, on average, at higher RH.

The results identified an RH rupture threshold in wheat pollen grains; once the ambient RH passes this threshold, rupture begins. Rupture does not occur as long as the ambient RH is below the threshold. Pollen grains rupture more quickly at a higher RH. The results demonstrate a relationship between pollen grain rupture and RH, and find the rupture is dependent on RH over time.

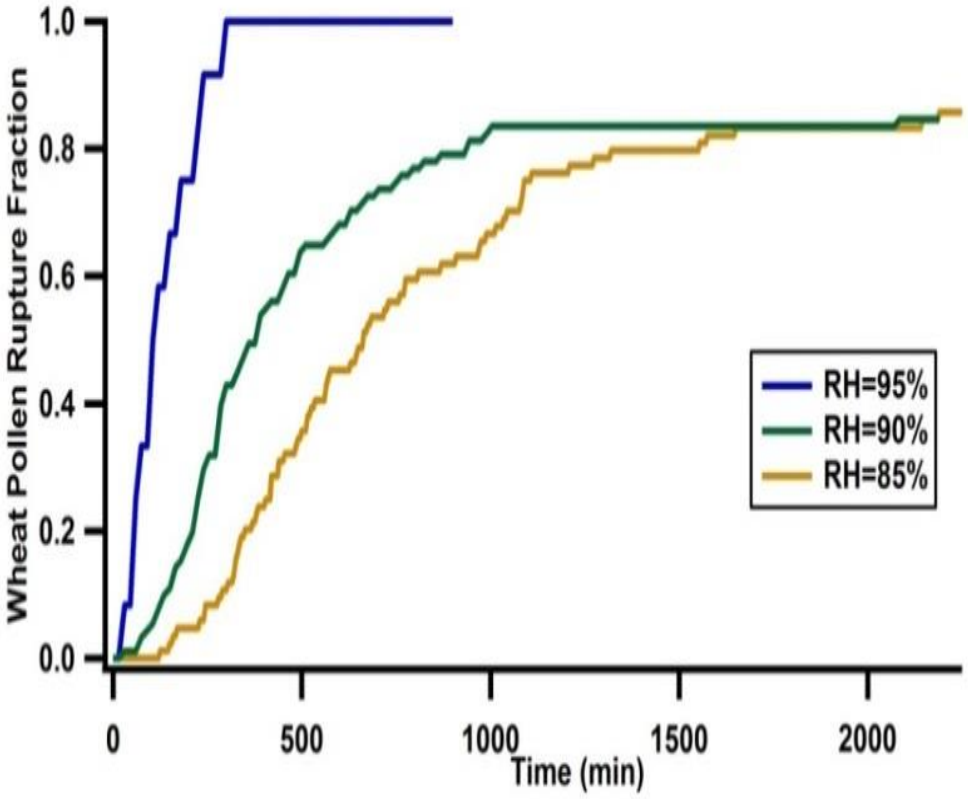

Figure 18. Cumulative pollen rupture fraction vs. time for all experiments

As discussed above, whether or not pollen will rupture is related to RH. Once RH exceeds the rupture threshold, the pollen grains rupture. Exposure to higher RH speeds pollen rupture. Alternatively, if the ambient RH is below the threshold rupture does not occur no matter how long the pollen is exposed RH. In dry areas (e.g., deserts) and in

winter, pollen can still rupture if the RH is saturated or over the threshold for a long period. Alternatively, in hot areas if the water vapor pressure is high and the RH is below the rupture threshold, rupture does not occur. From the standpoint of meteorological conditions, the pollen grains of some species rupture under high RH conditions such as dew or fog.

3.4 Ryegrass experiments

Ryegrass is important in lawns and pastures and is also a major allergen source. We have run experiments on other species including ryegrass and red pine. Results for these plants yielded different results from those on wheat pollen. No rupture was observed for red pine pollen (Fig. 19) even after hours of immersion in pure water. We speculate that the threshold for ryegrass pollen is higher than in wheat pollen, but it was difficult to maintain high RH using our device. However, preliminary results indicated diversity among various plant species. This may be due to variety in threshold water potential in pollen, size difference, pollen shell rupture strength, or pollen shell water permeability. The rupture pattern is another plausible factor. From the image analysis, we found that wheat pollen rupture originated from pollen shell cracks; while particles released by ryegrass pollen were found only near the tube pores. It is possible that ryegrass pollen is smaller and has a stronger shell. The pollen tube pores in the shell may be the only weak point where pollen rupture can occur in ryegrass.

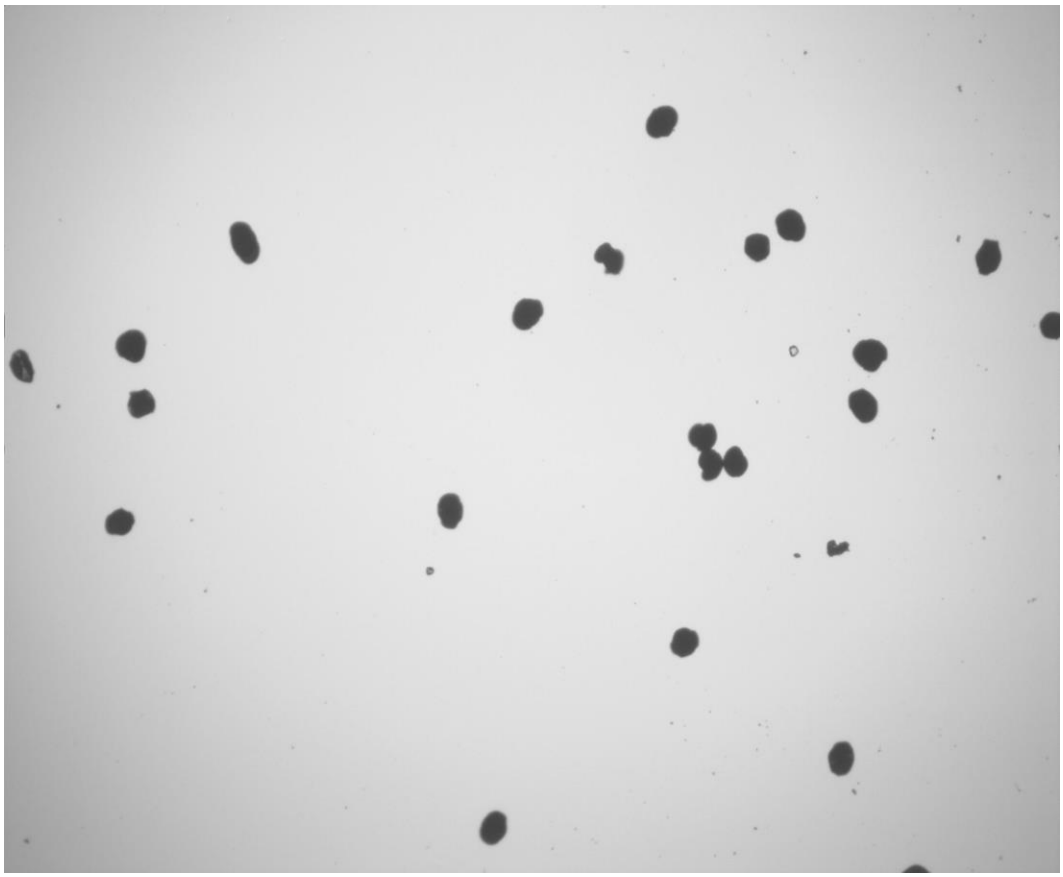

Figure 19. Red pine pollen experiments at RH=95% after 48 hours exposure

CHAPTER 4 : RUPTURE MODELING DEVELOPMENT

4.1 Purpose of Investigation

We propose that pollen rupture is caused by the water potential difference between ambient air and the pollen grain cytoplasm. Pollen grains absorb water because the substantial amounts of protein, starch, and other polysaccharides in pollen reduce the water potential of the pollen grain cytoplasm. Water always flows from overall high water potential (including pressure potential, gravity potential, osmotic potential, and matrix potential) to low water potential. When the air has greater water potential, pollen grains take up water, diluting the materials inside them and increasing their water potential; at this point, the pollen grains swell. The increase in volume is not unlimited, but is restricted by the shell. Even when the volume is unchanged, water flow into the pollen grain compresses the cytoplasm and increases turgor. Once the turgor pressure exceeds shell strength, the grain ruptures (Bolick & Vogel, 1992). If a rupture model can be developed using parameters from our experimental data, it will be possible to understand the conditions of pollen rupture. Combined with meteorological conditions, allergen dispersion can be predicted. This will help those with asthma know when to reduce outdoor activities to avoid inflammation of the airways.

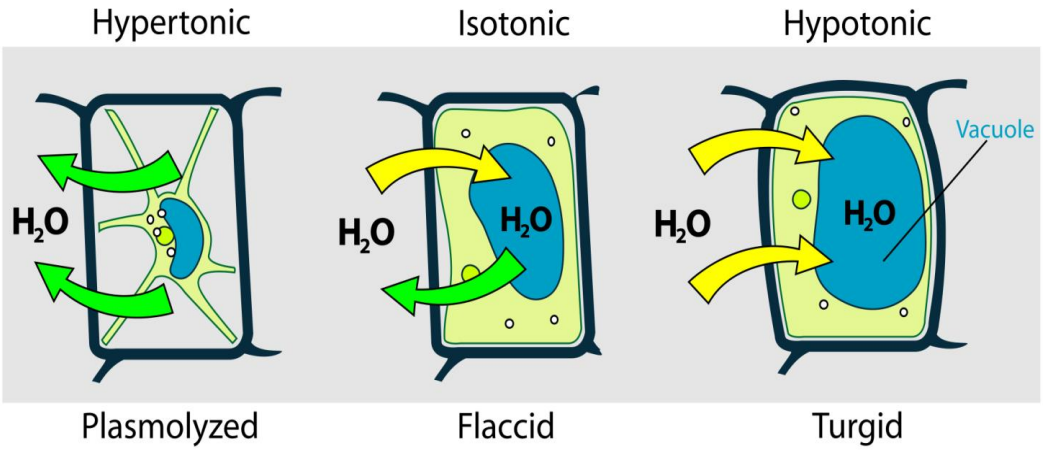

Figure 20. Water flux and turgor pressure changes in plant cells at various concentrations

(http://en.wikipedia.org/wiki/File:Turgor_pressure_on_plant_cells_diagram.svg)

Experiments were done on other species, however, pollen rupture was not observed with these species under our experimental conditions (Fig. 19). This indicates that pollen grains from various species have varying rupture patterns under the same water vapor conditions.

Pollen behaves differently in different species, suggesting variations in pollen cytoplasm water potential, water transport resistance in the pollen shell, pollen shell strength, pollen grain size, and maximum pollen grain expansion. Even pollen grains from the same species will have different diameters, potentially producing different rupture rates.

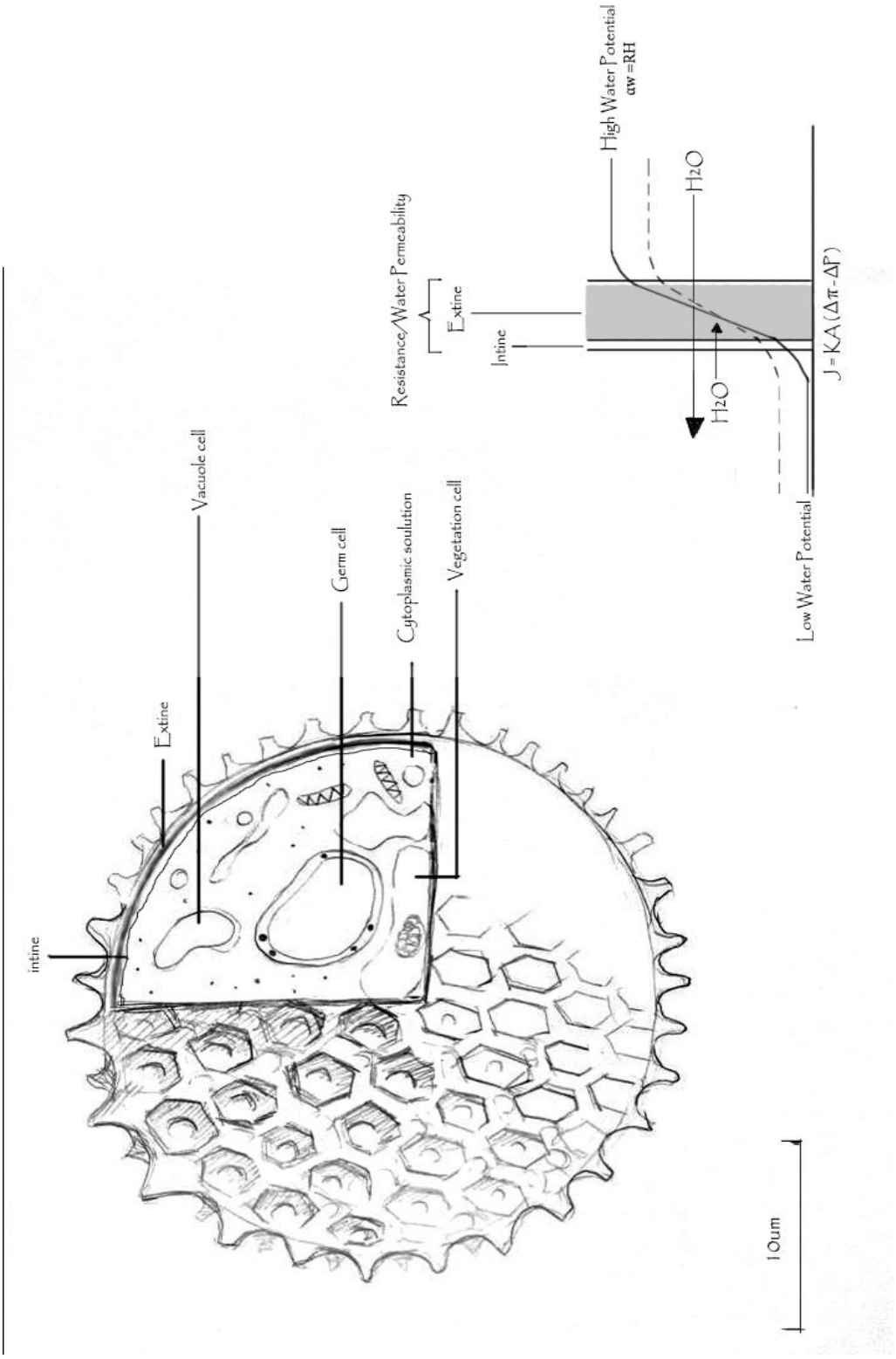

Figure 21. One quarter of a plant pollen grain

Pollen grains have a two layer shell (extine and intine) (Fig. 21). These layers protect the pollen and prevent water from moving freely into and out of the grains. Pollen grains contain organelles, germ cells, and vegetative cells; these are surrounded by cytoplasm. The cytoplasmic solution inside pollen can be viewed as adding protein, starch, and other polysaccharides to pure water. This process reduces the water potential of pure water. Water flows from higher water potential to lower water potential. The extine and intine stop macromolecules from moving, while still allowing water to flow with resistance. If the water potential of ambient air is higher than the water potential of the cytoplasmic solution, water will continuously enter the pollen. However, if the water potential of the ambient air is lower than that of the pollen's cytoplasmic solution, water will evaporate from the pollen. We can view the water potential of pollen cytoplasmic solution as the rupture threshold described previously.

Based on the previous results with wheat, and some preliminary experiments on ryegrass, we believe that changes in pollen grain morphology and the rupture process are induced by turgor changes (Fig. 20) due to water potential difference. The model development is based on a set of assumptions and parameters identified from the previous experimental data. It deals with water potential change (including osmotic potential and turgor pressure), which are the basic driving force in pollen rupture.

4.2 Equation development

The rate at which water enters the pollen grain depends on osmotic and turgor pressure differences, the water permeability of the pollen extine (pollen grain wall), and the pollen grain surface area

$$dV/dt = A_{sur}k(\pi_{out} - \pi_{in} - \Delta P) \qquad (1)$$

Where dV/dt is the rate of pollen grain volume increase (unit: $\mu m^3/s$), A_{sur} is the surface area of the pollen grain (unit: μm^2); k is the water permeability of the pollen grain shell (unit: cm⁄sMPa); π_{out} and π_{in} represent water potential outside and inside the pollen grain, respectively (unit: Pa); and ΔP is the pressure difference between turgor pressure in the pollen grain and atmospheric pressure (unit: Pa). The volume of the pollen grain will increase if $\pi_{out} - \pi_{in} - \Delta P > 0$ until the volume reaches the pollen grain's limit (approximately 1-2 μm larger than the normal radius, based on the wheat experiments). From equation (1), it can be seen that the volume change in pollen is related to the pollen radius, water permeability of the pollen wall, water potential difference between pollen and ambient air, and the pressure difference.

By rearranging equation (1), we get equation (2).

$$k = \frac{dV/dt}{A(\pi_{out} - \pi_{in} - \Delta P)} \qquad (2)$$

The water permeability can be calculated by equation (2).

The volume change over time is calculated by measuring swelling in the pollen grain. First, a glass slide with standard 100 μm length will be needed under microscope view; a measure tool is calibrated by measuring this length. The change in pollen diameter is then measured to calculate volume change. The pollen surface is calculated using the pollen diameter. Outside water potential is calculated from the RH of ambient air. The initial water potential inside the pollen can only be estimated by putting pollen in isotonic solution, however.

4.3 Assumptions

Assumptions need to be made before we explain the calculations. The pollen grains became slightly desiccated after they were harvested from the greenhouse. Therefore, at the beginning of each experiment they needed some time to uptake water from the atmosphere to return to normal moisture. After that, by adding water to the pollen grain, the volume of the pollen grain was increased. However, this volume expansion is not unlimited. From experimental observations, we identified 1-2 μm as a reasonable radius expansion value. After the grains reached maximum volume, water continued to enter the pollen, resulting in increased turgor pressure. This model cannot predict pollen swell and rupture directly. But by calculating the increase in turgor pressure over time, the trend of pollen rupture can be estimated.

The critical factor identified from the experimental results was water permeability. By measuring pollen volume change over time from the beginning when the pollen grain begins absorbing water, the water permeability of the wheat pollen wall was estimated as $k \approx 5.0 \times 10^{-9}$ cm⁄sMPa. To justify this estimate, water permeability was increased and decreased by factors of ten.

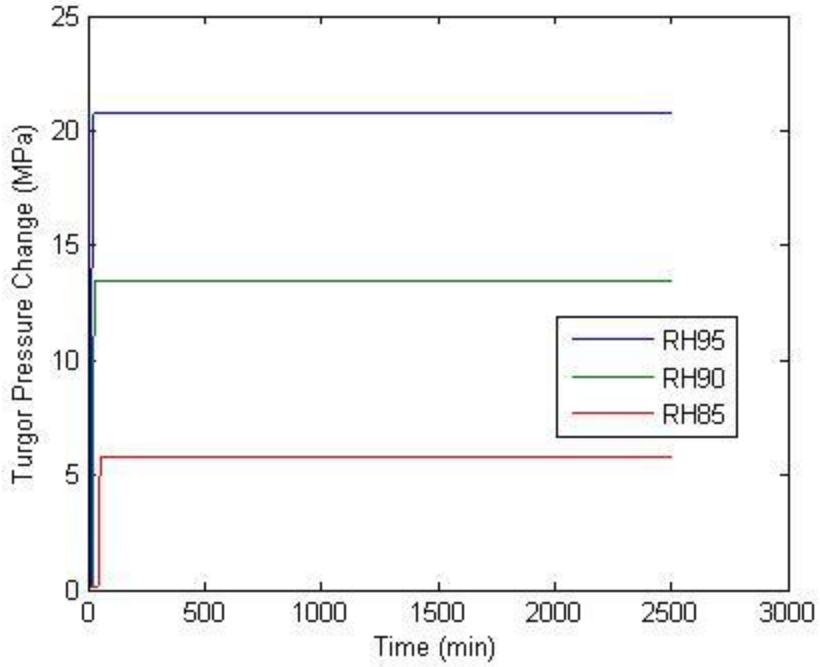

Figure 22. Simulated turgor pressure change when K is increased by a factor of ten

If water permeability is increased to a factor of 10, the pollen will have a very short time for expansion in the following model (Fig. 22).

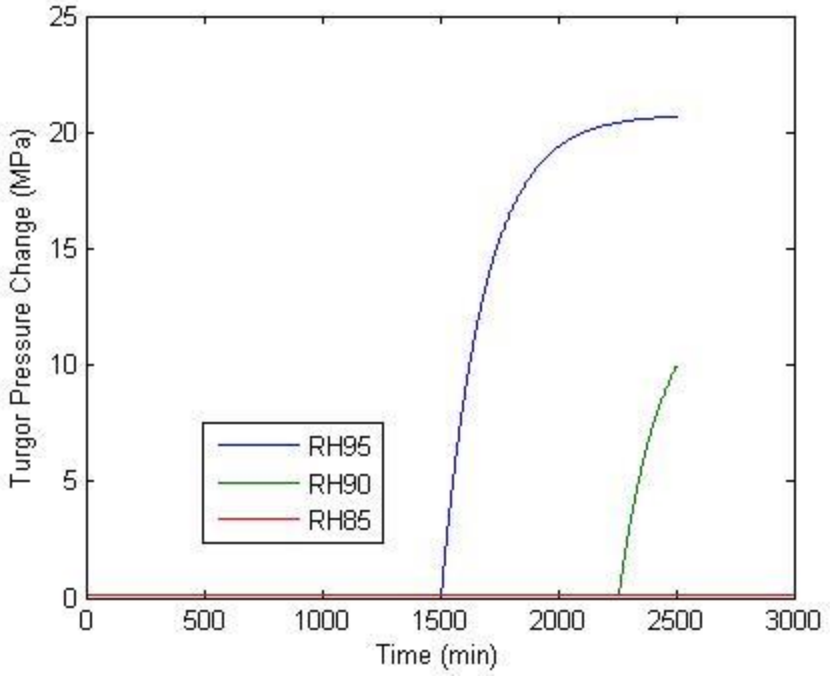

Figure 23. Simulated turgor pressure change where K is decreased by a factor of ten

However, if water permeability is decreased by a factor of 10, the pollen takes more than 48 hours to reach the desired expansion (Fig. 23). If water permeability is increased and decreased by factors of 100, the turgor pressure either reaches maximum pressure immediately, or accumulates no turgor pressure at all. The expansion time has been observed from experiments and these observations justify a water permeability range between $0.5\sim5.0\times10^{-9}$ cm/sMPa.

From the image analysis, we know that the wheat pollen grain radius has a range of 25 μm to 35 μm, with an expansion range of 1 μm to 2 μm. Other parameters needed for model development are identified from the experimental data. Room temperature is 22 ^{o}C; atmospheric pressure is a constant 0.917 atm. Water potential in the ambient air is

constant and calculated by $\pi = \frac{\mathrm{RT}\,(\ln RH)}{M_w}$ (RH=85%, 90%, and 95%) in each experiment. Through exposure to various RHs, the isotonic RH is used to estimate water activity in wheat pollen. In our experiment, the water activity in fresh wheat pollen was a_w=80%. This value is verified by exposing wheat pollen to a variety of ambient RH conditions. Pollen will desiccate if the ambient RH is below 80%; above 83% RH it takes in water and ruptures. There is no precise RH value at which all pollens remain stable, but it is believed that an RH range between 78~83% is a good estimate. Therefore, RH=80% is used to estimate pollen water potential in our model. Other researchers have prepared isotonic solutions close to this value to study pollen germination. Fig. 24 shows a comparison of experiments between exposed to RH=85% and RH= 82%. In fact, both of these two RH are supposed to be maintained at RH=85%. However, in one experiment, the RH control was below RH=83% in the beginning and no rupture were observed. After the RH increased and over 83%, the ruptured started. From this "bad" experiment, we hypothesize that there is a threshold RH for pollen to rupture. Once the ambient RH is over this threshold, pollen will rupture over a certain period of time.

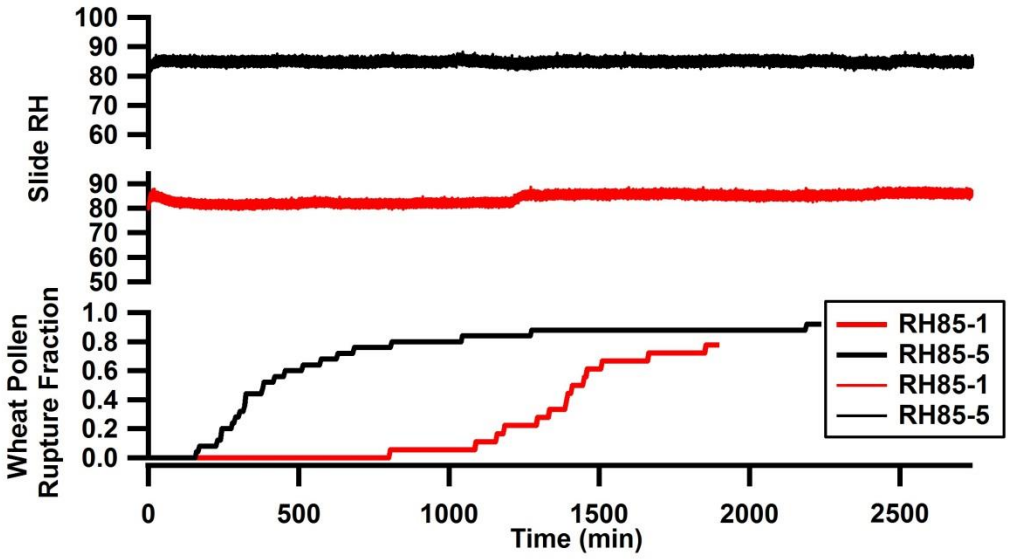

Figure 24. The discovery of a wheat pollen rupture threshold

4.4 Two Stage Inflated Model

In the first stage, turgor pressure in the pollen grain was the same as the atmospheric pressure (0.917 atm) ($\Delta P = 0$). Water potential in air is constant and calculated by $\pi = \frac{\mathrm{RT}\,(\ln a_w)}{M_w}$; while the water potential in the pollen grain is actively changing as water enters the pollen grain. At *t*=0, the osmotic potential in pollen is estimated by $\pi = \frac{\mathrm{RT}\,(\ln a_w)}{M_w}$ and a_w=80% (based on experimental observation). After the initial stage, the pollen grain's osmotic potential is calculated dynamically every 1 second (*dt*=1s) using the change in concentration in the solution ($C = -\frac{\pi}{RT}$, $CV = C_1V_1, V = V_1 + dV$, $\pi_1 = -C_1RT$). We then substitute the new value into Equation (1) to calculate the volume change in the pollen (*dV*) every 1 second. New values for osmotic potential, volume, radius, and so on are then calculated.

In the second stage, as the pollen grain is recovered to 1 μm to 2 μm larger than normal size, the pollen stops increasing in volume. Because the dV/dt is zero, equation (1) is not appropriate for stage two. Equation (3) is, therefore, introduced to replace equation (1) as:

$$J = A_{sur}k(\pi_{out} - \pi_{in} - \Delta P) \qquad (3)$$

The unit of water flux *J* over pollen surface is $\mu m^3/s$, and *J* is converted to dn/dt with a unit of mol/s during calculation. As water continuously enters the pollen grain, the density of the cytoplasmic solution is compressed and turgor pressure in the pollen increases.

The water solution can be compressed only a little. When compressed, the solution pressure increases as solution density increases. The ratio of pressure and density increase is defined as the bulk modulus. The bulk modulus measures the resistance of the solution to compression. In our experiment, the water bulk modulus has a value of 2.15×10^9 N/m^2.

In the second stage, the wall of the pollen grain confines water within it, while ambient water enters continuously. This increases the density of solution in the pollen grain and increases the turgor pressure. To calculate the turgor pressure, equation (4) is introduced.

$$p_1 = p_0 + E(1 - \frac{\rho_0}{\rho_1}) \qquad (4)$$

In this equation, p_1 is the final pressure (N/m2) after compression, ρ_1 is the final density (kg/m^3) after compression, p_0 is the initial pressure, and ρ_0 is the initial density

before compression. The bulk modulus fluid elasticity is represented by E; (N/m^2) represents resistance to uniform compression.

At t=0, water flux can be calculated in equation (3). The volume of pollen remains the same, so the turgor pressure increases according to equation (4). Furthermore, the water continuously enters pollen and dilutes the cytoplasm solution in the pollen grain than t=0. This reaction slows down dn/dt at time=1s, and the newly increasing turgor pressure and decreasing osmotic potential will reduce dn/dt at time=2s, and so on. Turgor pressure continuously increases as water enters the pollen grain. The pollen shell ruptures when pressure exceeds the shell's strength limits. Pollen cytoplasmic turgor pressure will stop increasing as $\pi_{out} - \pi_{in} - \Delta P = 0$. At this point, if turgor pressure has not reached the shell's critical rupture point, rupture does not occur.

However, there is a problem. In stage 2, it is assumed that the pollen volume will not increase and the solution inside the pollen is compressible. The solution concentration is supposed to be molarity to calculate osmotic potential. Because the volume is constant, the concentration does not change in molarity (it does change in mass). The calculation of osmotic potential is based on molarity and volume change (($C = -\frac{\pi}{RT}$, $CV = C_1V_1, V_1 = V + dV$, $\pi_1 = -C_1RT$)). The solution inside the pollen grain does not change concentration or volume in stage 2. At this point, further research is needed to develop a more reasonable calculation.

4.5 Simulated Results

This model will not directly forecast when pollen grains rupture; instead it estimates a reasonable turgor pressure trend in the pollen grain. To predict the pollen rupture, the strength of pollen grain wall should be better understood. From the simulated results, both pollen grain expansion and turgor pressure increase faster under higher RH at a pollen radius of 25~35 μm (Fig. 23). Larger pollen grains will reach higher turgor pressure than smaller grains. Based on images from the experimental phase, wheat pollen grains have an expansion range of 1~2 μm, this difference changes the times needed to start to increase turgor pressure and reach maximum turgor pressure (Table 2, 3, 4). Maximum turgor pressure is also affected by pollen radius and maximum expansion diversity. Generally, for a specific radius at the same expansion limit, exposure to higher ambient RH will start earlier to increase turgor pressure inside pollen. Under higher RH, the time needed for pollen to rupture is shorter and the ending turgor pressure is higher. As for pollen diameters, turgor pressure increases more quickly in larger pollen grains and reaches higher final turgor pressures. In our observations, larger pollen grains are likely to have larger expansion limit, thus required more time to accumulate turgor pressure, and will have higher ending pressure.

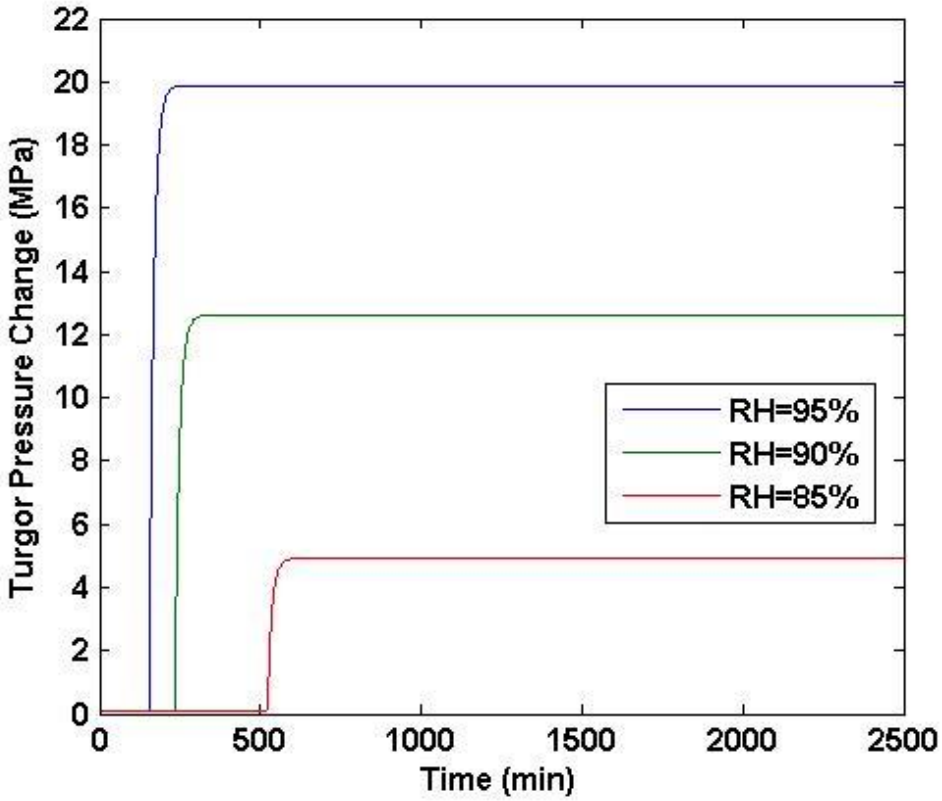
Turgor Pressure Change (MPa)
Time (min)
RH=95%
RH=90%
RH=85%
0
2
4
6
8
10
12
14
16
18
20
22
0
500
1000
1500
2000
2500

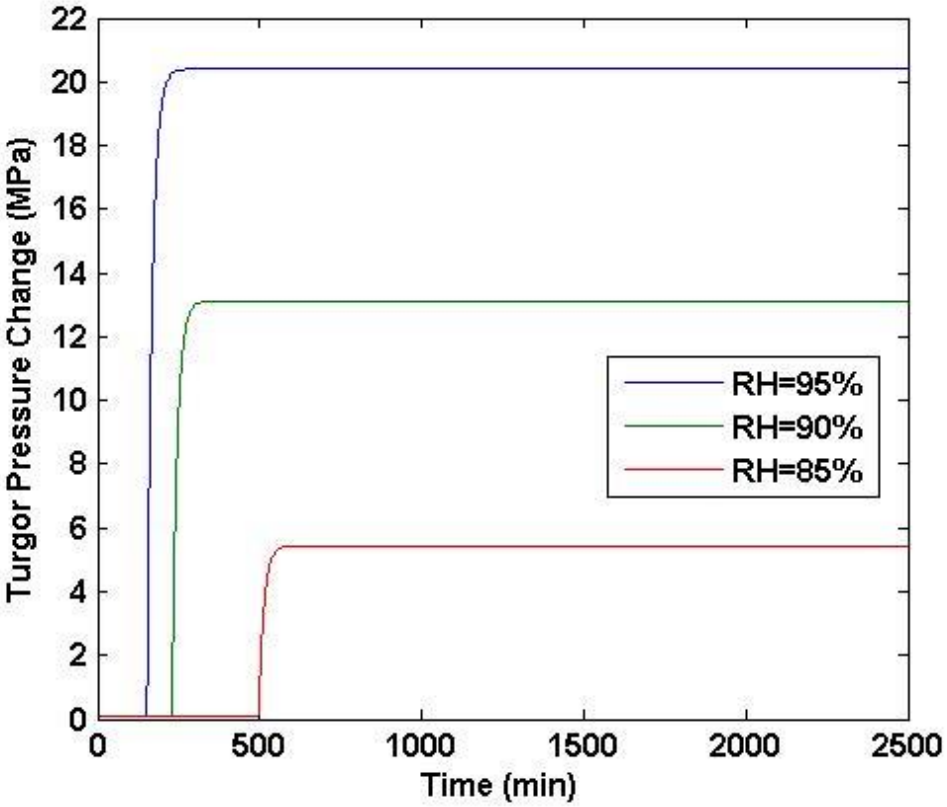
Turgor Pressure Change (MPa)
Time (min)
RH=95%
RH=90%
RH=85%
0
2
4
6
8
10
12
14
16
18
20
22
0
500
1000
1500
2000
2500

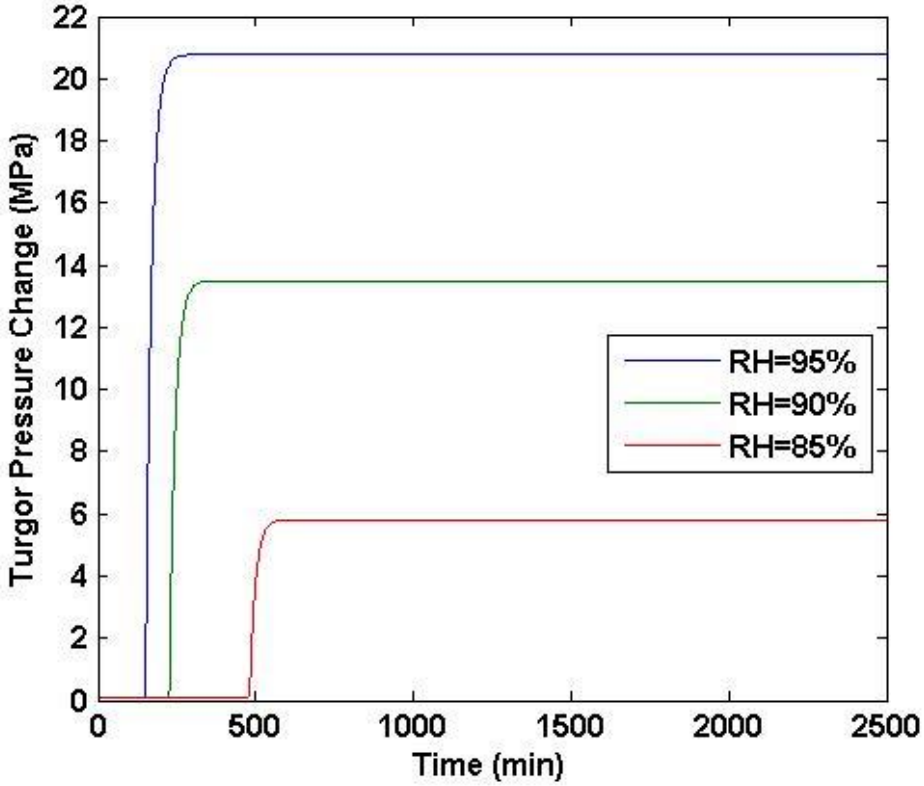

Figure 25. Predicted pollen grain turgor pressure change over time (From above to below radius 25, 30, and 35 μm, max radius expansion 1 μm)

Table 2. Time of turgor pressure to start to increase and reach max pressure under RH=85%, 90%, 95% (with pollen radius of 25, 30, and 35 μm, and max expansion radius of 1 μm)

1 μm	25 μm			30 μm			35 μm		
RH	85%	90%	95%	85%	90%	95%	85%	90%	95%
Start time/s	14830	2120	1190	11350	2060	1170	9910	2020	1160
MaxPressure Time/s	15370	3440	2260	12190	3620	2450	10990	3800	2670
Max Pressure/MPa	0.515	8.222	15.516	0.949	8.661	15.954	1.272	8.979	16.265

Table 3. Time of turgor pressure to start to increase and reach max pressure under RH=85%, 90%, 95% (with pollen radius of 25, 30, and 35 μm, and max expansion radius of 1.5 μm)

1.5 μm	25 μm			30 μm			35 μm		
RH	85%	90%	95%	85%	90%	95%	85%	90%	95%
Start time/s	N/A	3440	1860	N/A	3300	1820	26890	3200	1790
MaxPressure Time/s	N/A	4690	2960	N/A	4750	3140	27850	4930	3340
MaxPressure/MPa	N/A	6.987	14.282	N/A	7.592	14.887	0.331	8.044	15.336

Table 4. Time of turgor pressure to start to increase and reach max pressure under RH=85%, 90%, 95% (with pollen radius of 25, 30, and 35 μm, and max expansion radius of 2 μm)

2 μm	25 μm			30 μm			35 μm		
RH	85%	90%	95%	85%	90%	95%	85%	90%	95%
Start time/s	N/A	5010	2580	N/A	4720	2520	N/A	4520	2460
MaxPressure Time/s	N/A	6260	3770	N/A	6210	3940	N/A	6330	4020
MaxPressure/MPa	N/A	5.839	13.149	N/A	6.592	13.882	N/A	7.161	14.454

The pollen grains rupture as turgor pressure exceeds the strength of the grain wall. From our previous experimental results, higher ambient RH results in faster pollen rupture. This agrees with findings on changes in simulated turgor pressure. Pollen swelling is limited because the osmotic potential will decrease $\frac{dn}{dt}$ to zero. Experimental observations of pollen grain expansion similarly show a limit to the expansion radius.

We speculate that pollen grain wall strength is not a constant value, but has a range among the same type of pollen grains. Hence, as turgor pressure increases in the second stage, ruptures gradually occur. However, under higher RH leads to a faster average increase in turgor pressure coinciding with the cumulative pollen rupture fraction in Figure 18.

CHAPTER 5 : CONCLUSIONS

In this study, an exposure chamber has been built to finish the desired experiment. However, the RH control system is not reliable especially for RH higher than 90%. Temperature difference between exposure chamber and flow air line is a big issue for us. This difference will affect the accuracy of RH control, and pollen rupture is very sensitive to this RH difference. Our microscope system is also a big problem needed to be solved. First of all, the camera has a different channel to capture image than binocular eyepieces. The pollen number in eyepiece lens is much more than captured by camera which leads to very limited pollen number in each picture. Another issue is camera resolution is not high enough. This issue makes it difficult to capture pollen image especial when conducting experiment on pollen of smaller size. The magnification of our microscopic objective lens includes 4x, 10x, 40x, and 100x. For wheat pollen, 10x works very well while for ryegrass pollen 10x is not enough and 40x is huge. We may need a 25x objective lens which is not available for the type of microscope we used.

This study shows that ambient water potential is the critical driving force for pollen rupture. Pollen species, shell structure strength, water permeability, and pollen grain size are important factors in pollen rupture. Results indicate that the pollen under higher RH exposure has overall higher rupture fractions and requires less time to rupture. However, there is a diversity of pollen size. According to the modeling simulation, larger pollen requires less time to rupture, the time of starting to accumulate turgor pressure is also affected by expansion diameter. In our observations, larger pollen is likely to have large diameter which will increase the time need to rupture. A rupture model is being

developed to predict pollen rupture under different ambient RH conditions for different pollen sizes. These findings can be used to develop a large scale prediction model to forecast pollen particle concentration during meteorological change. Current and potential asthma patients will benefit from this model because it will help them to avoid exposure to allergens. To achieve this objective, more human health related plant pollens should be studied to identify parameters for a large scale model with meteorological conditions data. The current study has discovered a pathway to new research. However, the image analysis process is labor intensive and must be improved. As is, this step severely restricts the speed and progress of research. Parameters and constants of the rupture model also need to be improved to make the predicted turgor pressure change more suited to experimental observation.

BIBLIOGRAPHY:

Abou Chakra, O., Jean-Pierre, S., Rogerieux, F., Peltre, G., Senechal, H., & Lacroix, G. (2009). Immunological Interactive Effects between Pollen Grains and Their Cytoplasmic Granules on Brown Norway Rats. *World Allergy Organization Journal, 2*(9), 201 - 207.

Alderman, P., Sloan, J., & Basran, G. (1986). Asthma and thunderstorms. *Archives of emergency medicine, 3*(4), 260.

BarnabÁS, B., JÄGer, K., & FehÉR, A. (2008). The effect of drought and heat stress on reproductive processes in cereals. *Plant, Cell & Environment, 31*(1), 11-38. doi: 10.1111/j.1365-3040.2007.01727.x

Bolick, M., & Vogel, S. (1992). Breaking strengths of pollen grain walls. *Plant systematics and evolution, 181*(3-4), 171-178.

Celenza, A., Fothergill, J., Kupek, E., & Shaw, R. J. (1996). Thunderstorm associated asthma: a detailed analysis of environmental factors. *BMJ: British Medical Journal, 312*(7031), 604.

CHAN, T. L., & LIPPMANN, M. (1980). Experimental measurements and empirical modelling of the regional deposition of inhaled particles in humans. *The American Industrial Hygiene Association Journal, 41*(6), 399-409.

D'Amato, G., Liccardi, G., D'Amato, M., & Holgate, S. (2005). Environmental risk factors and allergic bronchial asthma. *Clinical & Experimental Allergy, 35*(9), 1113-1124. doi: 10.1111/j.1365-2222.2005.02328.x

Dabrera, G., Murray, V., Emberlin, J., Ayres, J. G., Collier, C., Clewlow, Y., & Sachon, P. (2013). Thunderstorm asthma: an overview of the evidence base and implications for public health advice. *QJM, 106*(3), 207-217. doi: 10.1093/qjmed/hcs234

Grote, M., Vrtala, S., Niederberger, V., Valenta, R., & Reichelt, R. (2000). Expulsion of allergen-containing materials from hydrated rye grass (Lolium perenne) pollen revealed by using immunogold field emission scanning and transmission electron microscopy. *Journal of Allergy and Clinical Immunology, 105*(6, Part 1), 1140-1145. doi: http://dx.doi.org/10.1067/mai.2000.107044

Masoli, M., Fabian, D., Holt, S., Beasley, R., & Global Initiative for Asthma, P. (2004). The global burden of asthma: executive summary of the GINA Dissemination Committee Report. *Allergy, 59*(5), 469-478. doi: 10.1111/j.1398-9995.2004.00526.x

Mauseth, J. (2009). *Botany: An Introduction to Plant Biology* (Fourth Edition ed.): Jones & Bartlett Learning, 2009.

Mukherjee, S., & Litz, R. E. (2009). Introduction: botany and importance. *The mango: Botany, production and uses*(Ed. 2), 1-18.

Packe, G., & Ayres, J. (1985). Asthma outbreak during a thunderstorm. *The Lancet, 326*(8448), 199-204.

Pan, L. J. (2006). *Response of Pollen to Electric Fields in Air.* Bachelor of Science, California Institute of Technology.

Pehkonen, E., & Rantio-Lehtimäki, A. (1994). Variations in airborne pollen antigenic particles caused by meteorologic factors. *Allergy, 49*(6), 472-477. doi: 10.1111/j.1398-9995.1994.tb00842.x

Rogerieux, F., Poncet, P., Sutra, J.-P., Peltre, G., Sénéchal, H., & Lacroix, G. (2010). Ability of pollen cytoplasmic granules to induce biased allergic responses in a rat model. *International archives of allergy and immunology, 154*(2), 128-136.

Schäppi, G. F., Taylor, P. E., Staff, I. A., Rolland, J. M., & Suphioglu, C. (1999). Immunologic significance of respirable atmospheric starch granules containing major birch allergen Bet v 1. *Allergy, 54*(5), 478-483. doi: 10.1034/j.1398-9995.1999.00838.x

Schäppi, G. F., Taylor, P. E., Staff, I. A., Suphioglu, C., & Knox, R. B. (1997). Source of Bet v 1 loaded inhalable particles from birch revealed. *Sexual Plant Reproduction, 10*(6), 315-323. doi: 10.1007/s004970050105

Suphioglu, C. (1998). Thunderstorm asthma due to grass pollen. *International archives of allergy and immunology, 116*(4), 253-260.

Suphioglu, C., Singh, M. B., Taylor, P., Knox, R. B., Bellomo, R., Holmes, P., & Puy, R. (1992). Mechanism of grass-pollen-induced asthma. *The Lancet, 339*(8793), 569-572. doi: http://dx.doi.org/10.1016/0140-6736(92)90864-Y

Taylor, P., & Jonsson, H. (2004). Thunderstorm asthma. *Current Allergy and Asthma Reports, 4*(5), 409-413. doi: 10.1007/s11882-004-0092-3

Taylor, P. E., Flagan, R. C., Miguel, A. G., Valenta, R., & Glovsky, M. M. (2004). Birch pollen rupture and the release of aerosols of respirable allergens. *Clinical & Experimental Allergy, 34*(10), 1591-1596. doi: 10.1111/j.1365-2222.2004.02078.x

Taylor, P. E., Flagan, R. C., Valenta, R., & Glovsky, M. M. (2002). Release of allergens as respirable aerosols: A link between grass pollen and asthma. *Journal of Allergy and Clinical Immunology, 109*(1), 51-56. doi: http://dx.doi.org/10.1067/mai.2002.120759

Taylor, P. E., Jacobson, K. W., House, J. M., & Glovsky, M. M. (2007). Links between pollen, atopy and the asthma epidemic. *International archives of allergy and immunology, 144*(2), 162-170.

Vaidyanathan, V., Miguel, A. G., Taylor, P. E., Flagan, R. C., & Glovsky, M. M. (2006). Effects of Electric Fields on Pollen Rupture. *The Journal of allergy and clinical immunology, 117*(2), S157.

Wardman, A. D., Stefani, D., & MacDonald, J. C. (2002). Thunderstorm-associated asthma or shortness of breath epidemic: a Canadian case report. *Canadian respiratory journal, 9*(4), 267-270.

Wilson, A. F., Novey, H. S., Berke, R. A., & Surprenant, E. L. (1973). Deposition of inhaled pollen and pollen extract in human airways. *The New England journal of medicine, 288*(20), 1056.